# AN ABSTRACT OF THE THESIS OF

Atanas A. Atanasov for the degree of Master of Science in Mechanical Engineering
presented on May 27, 2014.

Title: Characterization and Mitigation of Train Vibrations in a Laboratory Facility

Abstract approved: _____
John P. Parmigiani

Excessive environmental vibrations can have deleterious effects in a variety of animals. Despite the potentially detrimental effects vibrations may have on animal health and experimental results, they remain poorly understood in the animal laboratory setting. This study investigates the consequences of excessive train vibrations on the breeding success of laboratory mice. An instrumented cage, featuring a high sensitivity microphone and accelerometer, was used to characterize the vibrations and noise in a vivarium that is in close proximity to an active railroad. The passing trains cause vibrations of a magnitude that is three times larger than the ambient vibrations caused by the mice. The majority of the noise recorded within the laboratory facility was below the audible range of mice and was thus considered to not have a significant effect on them. To verify the effect of the train vibrations, a controlled vibration study was conducted by using a custom-built electromagnetic shaker to simulate the train vibrations. Mice, which were unaccustomed to train vibrations, served as the test subjects and were vibrated in a facility far from the railroad tracks. The stress levels of the mice test groups, featuring both males and females, were compared to control groups in order to establish the significance of the results. It was determined that vibrations similar to those produced by a passing train can create large fluctuations in the stress levels of female mice. These fluctuations in stress levels warrant concern due to the negative effects that stress can have on mice and, consequently, on experimental outcomes. In order to alleviate further negative impacts on laboratory research, a vibration isolating caster system was designed to replace the one currently being used on the flat, wire racks on which the mouse are housed.

# Characterization and Mitigation of Train Vibrations in a Laboratory Facility

by

Atanas A. Atanasov

A THESIS

submitted to

Oregon State University

in partial fulfillment of
the requirements for the
degree of

Master of Science

Presented May 27, 2014
Commencement June 2014

Master of Science thesis of Atanas A. Atanasov presented on May 27, 2014.

APPROVED:

---

Major Professor, representing Mechanical Engineering

---

Head of Mechanical, Industrial and Manufacturing Engineering

---

Dean of the Graduate School

I understand that my thesis will become part of the permanent collection of Oregon State University libraries. My signature below authorizes release of my thesis to any reader upon request.

---

Atanas A. Atanasov, Author

# ACKNOWLEDGEMENTS

First and foremost, I would I like to thank Dr.John Parmigiani for granting me the opportunity to change course and become a mechanical engineer. I have learned much in my time as a graduate student, which would not have been possible without Dr.Parmigiani's encourgement and willingness to allow me to pursue a variety of projects and coursework. I cannot find the words to explain the appreciation I have for my family. They have been an unconditional source of love and support during my graduate students and my life in general. I also could not ask for better friends, their companionship and mentorship have made me a better individual and have helped me always see the glass half full. Last but certainly not least, I would like to thank everyone that has shaped this study and aided in making it a reality, including Dr.Helen Diggs, Jennifer Grossman, Rupert Palme, Edith Klobetz-Rassam, James Batti, and all of the LARC staff.

# TABLE OF CONTENTS

Page

1 Introduction 1

1.1 On the care of Laboratory Animals . . . . . 1

1.2 Noise and Vibration as Biological Stressors . . . . . 1

1.3 The Laboratory Animal Resources Center and the Problem Within It . . . 3

1.4 Goal of this study . . . . . 5

2 Vibration and Noise Characterization 6

2.1 Basic Theory of Vibration and Sound . . . . . 6

2.2 Facility Description . . . . . 7

2.3 Measurement Cage . . . . . 8

2.4 Data Analysis and Statistical Methods . . . . . 10

2.5 Results and Discussion . . . . . 12

2.5.1 Results . . . . . 12

2.5.2 Discussion . . . . . 16

3 Laboratory Stress Study 18

3.1 Facility and Description . . . . . 18

3.2 The Stress Study . . . . . 18

3.3 Electromagnetic Shaker . . . . . 20

3.4 Mice . . . . . 22

3.5 Data Analysis and Statistical Methods . . . . . 22

3.6 Results and Discussion . . . . . 23

3.6.1 Results . . . . . 23

3.6.2 Discussion . . . . . 26

4 Mitigation of Train Vibrations 28

4.1 Basic Theory of Vibration Isolation with Applications to this Study . . . . 28

4.2 System Characterization . . . . . 32

4.3 Isolator Design . . . . . 35

4.3.1 Assuming a Simplified Model and the Transmissibility Plot . . . . 36

4.3.2 Isolator Device Selection and Design . . . . . 38

4.4 Future Work and Suggestions . . . . . 57

# TABLE OF CONTENTS (Continued)

Page

5 Conclusion 59

5.1 Summary of Work . . . . . 59

5.2 Impact of Study . . . . . 60

5.3 Final Remarks . . . . . 60

Bibliography 60

Appendices 64

A Matlab Code . . . . . 65

B Structural Stability Calculation: Elastomeric Isolator . . . . . 69

# LIST OF FIGURES


| Figure | | Page |
|---|---|---|
| 1.1 | Location of the LARC and, specifically, room 103 (shown in black) | 4 |
| 2.1 | Example of a sinusoidal wave | 7 |
| 2.2 | Measurement cage | 8 |
| 2.3 | Typical vibrations within room 103 with mice on the flat rack | 13 |
| 2.4 | Typical vibrations within room 103 without mice on the flat rack but with equivalent weight added | 14 |
| 2.5 | Typical acceleration from LPSC room 62 | 15 |
| 2.6 | Typical Leq of room 103 | 15 |
| 3.1 | Top and side view of the electromagnetic shaker | 21 |
| 3.2 | Plot of averaged FCM levels in the female mice group | 23 |
| 3.3 | Plot of averaged FCM levels in the male mice group | 24 |
| 3.4 | Plot of combined average FCM levels in the female mice group | 24 |
| 3.5 | Plot of combined average FCM levels in the male mice group | 25 |
| 4.1 | Example of equivalent mass-spring system | 30 |
| 4.2 | Sample transmissibility plot | 31 |
| 4.3 | Sample transmissibility plot | 34 |
| 4.4 | Transmissibility curves for medium and high load values | 37 |
| 4.5 | Flowchart outlining the selection/design process of the vibration mitigating device | 39 |
| 4.6 | Load versus displacement curve for new casters | 41 |
| 4.7 | General isolation system assembly | 42 |
| 4.8 | Helical wire isolator | 44 |

# LIST OF FIGURES (Continued)

Figure Page


4.9 Pneumatic elastomeric isolator . . . . . 45

4.10 Pneumatic elastomeric isolator. Courtesy of McMaster-Carr. . . . . 47

4.11 Pneumatic elastomeric isolator load versus displacement plot . . . . . 48

4.12 Moment being generated due to rack loading . . . . . 50

4.13 Example load versus displacement plot of a typical elastomeric material, hysteresis is noted. As adapted from [30] . . . . . 52

4.14 Selected elastomeric isolator. Courtesy of Advanced Antivibration Components. . . . . 53

4.15 Load versus displacement curves for elastomeric mounts. Courtesy of Advanced Antivibration Components. . . . . 54

4.16 Free body diagram of a single caster . . . . . 55

4.17 Final elastomeric isolator assembly . . . . . 56

# LIST OF TABLES


Table Page

3.1 Summary fecal collection and vibrations times . . . . . 19

4.1 Summary of original rack characteristics . . . . . 35

4.2 Comparison of criteria for isolator selection . . . . . 40

4.3 Pneumatic isolator specifications . . . . . 47

4.4 Stiffness and transmissibility characteristics of pnuematic isolator . . . . . 49

4.5 Natural frequencies of pneumatic isolator system . . . . . 49

# Chapter 1: Introduction

## 1.1 On the care of Laboratory Animals

Laboratory mice are the most commonly used mammal for biomedical research in the United States [19]. The small size of the mice, in addition to their fast reproductive capabilities and similarity to humans, makes them an ideal research animal. The conditions under which the mice are kept and research is conducted are closely controlled in regards to air quality, relative humidity, temperature, and light cycles. Mice are usually housed in a group in cages which are either placed on flat, wire racks or ventilated rack units. Most cages are made of plastic and contain bedding, water, and food for the animals. The cages and the routine involved in cleaning them are regulated in order to maintain research standards. The standards are administered by the Public Health Service. In certain facilities, the Association for Assessment and Accreditation of Laboratory Animal Care International also specifies standards. The controlled laboratory environment of the mice, however, lacks requirements for noise and vibrations. The Guide for the Care and Use of Animals suggests that noise and vibration in animal research facilities should be reduced if possible [8]. The lack of standards for noise and vibration is problematic because an excess of either noise and/or vibration may serve as a drastic stressor to mice.

## 1.2 Noise and Vibration as Biological Stressors

Noise and vibrations in laboratory facilities are not, as of this writing, officially standardized or monitored phenomena in the United States. However, the presence of noise and vibrations has been observed to affect the behavior and biological response of a variety of mammals. Noise, as it relates to rodents, has been studied to a greater extent than vibrations and tends to be more well understood by the scientific community.

Noise can have numerous effects on rodents and is studied to a larger extent as compared to vibrations, possibly because it is a more readily observable phenomena. It

is important to understand, however, that noise as perceived by humans differs from what is experienced by a mouse. Humans have the capability to hear sounds ranging from 20 Hz to 20,000 Hz while mice hear in the range of 1000 Hz to 100,000 Hz [13]. The difference in hearing ranges between humans and mice may cause investigators to have concern over noise that cannot even be heard by mice or may cause neglect of noise problems that may exist which are beyond the hearing range of humans. Such conclusions have been documented by Reynolds, et al. who investigated the noise produced by ventilated rack units, construction equipment, and animal transfer stations. Reynolds, et al. determined that much of the noise perceived by humans was not audible to mice due its low frequency characteristics [32]. Prolonged exposure to excessive noise(90 dB - 110 dB) within the hearing range of mice has been documented to cause decreased birth rates, an increased number of stillborn pups, increased heart rates, increased arterial pressure, a reduction in response of the parasympathetic nervous system, and increased inflammation in the intestinal mucosa [31, 3]. Excessive noise can be problematic in an animal facility if the noise is within the hearing range of mice and if it is excessive, greater than 90 dB; However, noise in many vivaria does not reach such levels and may not be a severe stressor for the animals. Unlike noise, the correlation between excessive vibrations and the physiological response of mice is far less explored.

Vibrations in animal facilities are not specifically monitored or accounted for. The lack of vibrations control in animal facilities may result in skewed experimental results and may even lead to poor animal health. No published data currently exists on the perception mice have of environmental vibrations; however, several studies elaborate on the possible effects certain vibrations may have on rodent physiology. Plasma corticosterone and brain serotonin levels have been observed to increase with vibrations of 0.4 $g$ at 20 Hz [2]. At amplitudes of 2.0 to 2.4 $g$ and 5 to 15 Hz in frequency, increased adrenal weight and decreased gastric emptying time have been noted [35, 36]. Whole body vibrations in mice have been seen to promote increased bone formation and also suppress adiposity, or animal fat stored in fatty tissue [34, 39, 40]. It is important to note that, though increased bone formation and decreased fat storage are positive effects, they have been noted to occur at vibrations of 0.1 to 0.3 $g$ and with a relatively high frequency (45-90 Hz) [34, 39, 40]. Furthermore, in terms of reproductive success, fetal resorption and potential for increased cleft palate have been noted in mice exposed to an earthquake that ranges 8-9 on the Richter scale. The mice stimuli were designed to repli-

cate an earthquake that occurred on March $2^{nd}$, 1985 in Santiago, Chile [21]. Increased levels of stress and a higher risk of cardiovascular problems has been noted by studies in which vibrations of 1 to 2.5 Hz have been administered through a shaker [6, 7, 23]. Shaker stress and vibrations have been noted to cause changes in blood pressure, heart rate, secretion of stress hormones, and sympathetic activity [12]. Though research has been conducted in regards to the affect of vibrations on mice physiology, more studies are needed to encompass the various vibration scenarios that occur in a laboratory setting [29].

## 1.3 The Laboratory Animal Resources Center and the Problem Within It

Laboratory animal vivaria are constructed to suit the needs of the institution in regards to proximity to other research facilities, campus land use planning, and land restrictions. As a result, laboratory animal housing may be located near subways, trains, or highways, all of which may transmit vibrations at a magnitude and frequency that could cause for elevated stress within rodents. The Laboratory Animal Resources Center (LARC) at Oregon State University (OSU) is located approximately 30 meters from an active railroad track. The LARC building has housed rodents, rabbits, and dogs at various times although the facility is currently used for rats and mice. The facility was built in the 1970s and is not designed to meet the needs of contemporary rodent research. Though the facility has undergone a minor retrofit, its exposure to environmental vibrations has never been evaluated. On average, four trains of varying lengths pass the building each day. The location of the passing train tracks in relation to the LARC is indicated in Figure 1.1.

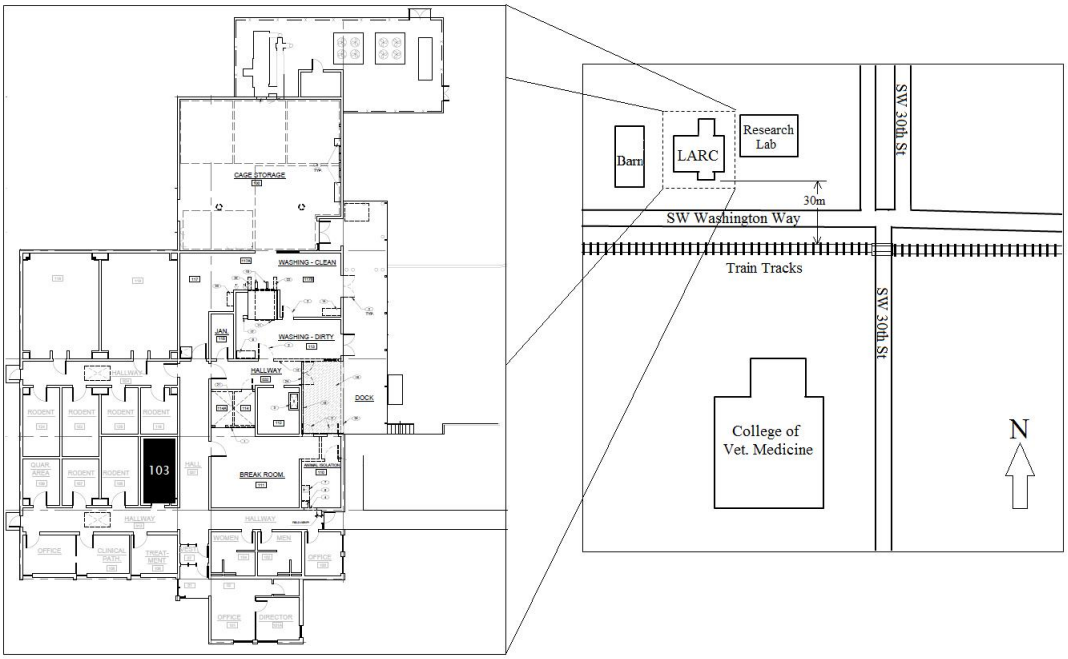


Figure 1.1: Location of the LARC and, specifically, room 103 (shown in black)

The LARC has been notorious for poor reproductive success and a certain strain of mice has even been noted to cannibalize their young. The most problematic location within the LARC appears to be room 103, which is the closest animal room to the train tracks. After investigating other potential causes such as temperature variations, light/dark cycles, and diet, it was hypothesized that the vibrations from the train could be a significant factor. The reproductive success of the same set of mice improved after they were moved from a flat wire rack (InterMetro Industries Corporation) to a single motor ventilated rack (Lab Products Inc, Super Mouse 1800). The ventilated racks are designed to hold cages in place with a cage clip and may, therefore, permit less cage-to-rack vibration. Ventilated racks are also much heavier and have an air intake and exhaust system which generates its own minor background vibrations, these factors may contribute to damping or partially masking the train vibrations. The reproductive success of mice in another animal housing facility on campus, the Linus Pauling Science Center (LPSC), is much higher than at the LARC. The LPSC is a state-of-the-art science

facility constructed in 2011 and is located approximately 490 meters away from the railroad tracks. The fluctuation in mouse reproductive success between facilities and rack types encouraged this investigation.

Measurements were taken initially within several rooms and on various rack types; however, it became apparent that each room and rack type had its own distinct response to the vibrations. In order to simplify the study and focus on the most problematic room with the most standard rack, room 103 was selected for the majority of the measurements and a flat, wire Super Erecta rack (InterMetro Industries Corporation) was used. Ventilated rack types differ widely from vendor to vendor and even within a single facility. Some ventilated racks have several ventilation motors, others only one, and thus cause their own vibrations that can convolute measurements. Vendors racks weigh different amounts which cause the vibration characteristics of the rack to vary. The study was designed to limit the amount of variables that influence the measurements.

## 1.4 Goal of this study

The specific goals of this study are to characterize the effects of train associated vibration and noise on laboratory mice housed on flat racks in the Laboratory Animal Research Center (LARC) and to develop ways in which to mitigate these stressors if they have an effect. Noise was monitored throughout the study to characterize its potential as a stressor and to possibly disregard its influence altogether. To explore the effects of train vibrations in a quantifiable manner, a study was conducted in which a set of mice were vibrated under controlled settings. To create controlled vibrations, an electromagnetic shaker was designed and constructed. The shaker was used to induce vibrations similar to those produced by passing trains at the LARC. The stress of the vibrated mice was monitored throughout the day and into the night by conducting a fecal corticosterone metabolite (FCM) analysis. It is hypothesized that mice exposed to train vibrations have fluctuating corticosterone as measured in FCM. Fluctuating FCM levels result in reduced reproductive success and lower pre-weaning pup survival. The final part of this study is manifested in the design and manufacture of a solution for any of the quantifiable stressors. The design process includes a description of several possible solutions and narrows the selection to the best that serves the situation.

# Chapter 2: Vibration and Noise Characterization

## 2.1 Basic Theory of Vibration and Sound

Vibrations and noise are two very similar phenomena, the major difference being the medium through which either the vibration or acoustic waves travel. Vibrations and noise can be thought of as propagating or traveling waves. Waves are initiated by a source causing a disturbance in the medium, e.g., an oscillating speaker cone which creates periodic compressions and dilatations of the surrounding air particles. The movement of the speaker cone creates waves which transfer energy through the medium, though the medium itself does not move as a whole [29]. Waves oscillate with a certain frequency and have particular amplitudes, which change as the waves propagate from the source. Figure 2.1 illustrates the key aspects of a wave; a sine wave is used for simplicity.

In Figure 2.1, $A$ indicates the amplitude, or maximum displacement of the wave. $T$ is the period of the wave, the time it takes for one cycle to complete or for the wave to repeat itself. The period is related to the frequency of the wave by the following formula: $f = 1/T$. For this study, it is important to know the frequency and amplitude of the waves that are measured in order to be able to categorize their effects. Certain wave frequencies and amplitudes may be more detrimental to the health of the mice. There are many types of waves; however, the majority of the energy produced by trains moving on the ground surface is conveyed by Rayleigh waves [27]. Such waves are usually of a frequency between 4-30 Hz, a range that can agitate people and lead to increased building damage [24, 27]. Regarding sound, the waves are similar to vibration waves except that the sound waves carry energy through the air, or water in some cases. Sound waves are pressure waves that longitudinally oscillate through the air. The ears of humans and mice are designed to respond to the sound pressure variances, which are consequently deciphered within the brain. The range of sound amplitudes that humans and mice can hear is vast; therefore, a logarithmic system exists than can conveniently capture such fluctuations. The decibel scale is used to indicate sound pressure in a more concise manner by setting the zero of the scale to the threshold of human hearing, 20 $\mu Pa$ [29].

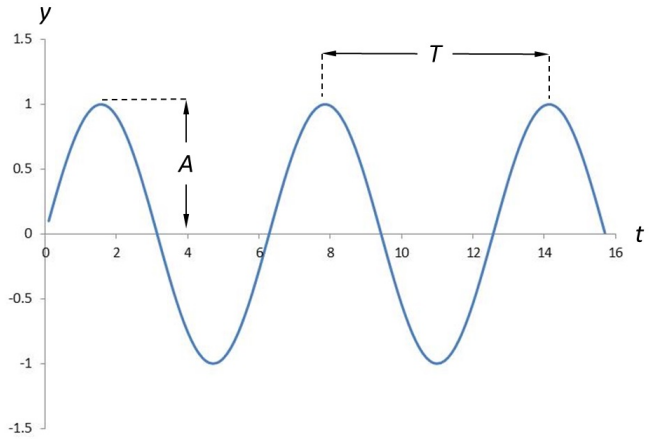


Figure 2.1: Example of a sinusoidal wave

Equation 2.1 indicates how the decibel scale is computed [5].

$$L_p = 10 * log(\frac{p^2}{p_{ref}^2}) \tag{2.1}$$

In Equation 2.1 above, the $p_{ref}$ value is taken to be the standard sound pressure level of 20 $\mu Pa$ and $p$ is the measured sound pressure. Noise and vibrations are complicated phenomena to study because their presence is influenced by a myriad of factors; however, they must be thoroughly investigated because their effects can be detrimental to laboratory studies.

## 2.2 Facility Description

The LARC was built in the mid-1970s and features interior and exterior walls constructed primarily of reinforced concrete masonry units (CMU). The ceiling is made of suspended gypsum board and the building floor is comprised of a concrete slab. The building is located roughly 30 meters from an active railroad and is not adequately retrofitted to account for excessive vibrations. The room which mice have historically had a low reproductive success in, room 103, is located on the corner of a hallway and is directly exposed to the train vibrations.

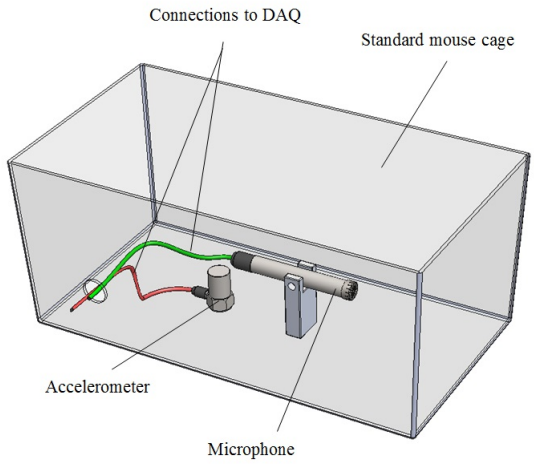


Figure 2.2: Measurement cage

## 2.3 Measurement Cage

To assess the presence and impact of environmental vibrations within the LARC, a measurement cage was created. The measurement cage consists of a SuperMouse 750 laboratory mouse cage, a vertically placed Kistler 8612B5 high sensitivity accelerometer, and a PCB 378B02 high precision microphone. Two pouches of water were placed within the cage in order to simulate an average cage mass of 2 kg. The bedding and other animal accessories were deemed to be unnecessary because the accelerometer is solely influenced by the mass of the cage and the incoming vibrations. The measurement cage connects to a National Instruments (NI) data acquisition unit (DAQ) which is used to relay the sound and vibration data to a Dell Vostro 1510 laptop equipped with LabVIEW data logging software. The NI DAQ system features a NI 9233 module and a NI cDAQ universal serial bus chassis. The system was used to measure the vibrations and noise present within the LARC and LPSC. A diagram of the system is displayed in Figure 2.2. The cage in Figure 2.2 has a cage lid; however, it is not displayed in the diagram.

The cage was equipped with a high precision microphone in order to detect the noise levels within the room. The noise measurements indicate whether excessive noise is a potential disturbance to the mice. The noise measurement sampling rate was set at 40

kHz in order to capture all noise frequencies up through 20 kHz, the maximum frequency that can be heard by the human ear. Though mice can hear noise above 20 kHz, it was deemed highly unlikely that anything within the facility would generate such high frequencies as per data from preliminary measurements. The vibration measurements were collected at a rate of 2 kHz, which amounts to a maximum frequency extrapolation of 1 kHz. A lower frequency value was used for vibration collection because vibration levels with frequencies higher than 1 kHz were not observed during an initial survey of the room. Vibration and noise measurements were collected on flat racks from 1pm to 5pm daily. In order to verify the passing of the train and to relate it to the observed vibrations and noise, a network camera (Q16 series, Axis Communications) was installed on one of the windows facing the railroad tracks. Using the video camera, video recordings were taken throughout the entire period of time in which vibration and noise measurements were collected.

Five measurements were taken with mice placed on the flat rack in order to provide a general understanding of the vibrations and noise that were present. In order to assess the frequency of the passing train with more accuracy, the vibrations on the flat rack, which were caused by the movement of the mice, had to be limited. Mice were removed from the rack and equivalent weight was added to the rack to match that of the mice in cages. The average mass of a mouse cage is 2 kg; thus, 20 weights were used that were each between 1.78 and 2.18 kg. The weights were spaced as if they were cages: uniformly on each level of the flat rack. Five measurements were taken with the weighted rack. The flat rack was chosen because it is a common, nationally and internationally used rack, it has less moving components (as compared to a ventilated rack), and, from initial findings, seems to be more susceptible to environmental vibrations. In addition to vertical measurements taken with the accelerometer, horizontal vibration measurements were also taken in order to determine their significance.

Measurements of horizontal vibrations were taken by fastening the accelerometer on a rigid metal L-bracket and securing it to the bottom of the instrumented mouse cage. Readings were taken in the same manner as the measured vertical vibrations.

In order to verify that the train vibrations were specific only to buildings in the immediate vicinity of the railroad tracks, a rack in an empty animal room in the LPSC was analyzed with the instrumented cage. The noise and vibration measurements followed the same procedures as those used in the LARC.

## 2.4 Data Analysis and Statistical Methods

All the vibrations and noise data was compiled and analyzed using Matlab, a mathematical software package by MathWorks, and the built-in capabilities of the LabVIEW software, a data collection and analysis software by NI. A Matlab script was written which plotted the vibration and noise data and extracted peak accelerations and sounds. The vibration data was collected in units of gravitational acceleration (g) while the noise data was measured in units of decibels (dB). The unit g correlates to 9.81 $m/s^2$ of acceleration. The units of dB were used to represent the collected sound pressure values on a logarithmic scale and in relation to a specific reference value.

For detailed information on measuring sound in a laboratory setting, refer to the publication by Hughes [14]. The noise measurements were further refined by computing the equivalent continuous sound level ($L_{eq}$) for every second of noise data. The $L_{eq}$ serves as a logarithmic average of the noise data and can be used to illustrate trends in sound levels over time; it is computed by Equation 2.2 below [5]. The $L_{eq}$ was calculated for every second of sound data, i.e. the time range over which the integration is taken is one second. The individual $L_{eq}$ calculations were then pieced together to form an equivalent sound level plot for the entire time range of the noise recordings.

$$L_{eq} = 10 * log \left\{ \frac{1}{T} \int_0^b \left( \frac{p_{A(t)}}{p_{ref}} \right)^2 dt \right\} \tag{2.2}$$

In Equation 2.2, $T$ is the total time of the increment over which the integral is taken, $p_{A(t)}$ is the instantaneous value of sound pressure, and $p_{ref}$ is the reference sound pressure (20 $\mu Pa$).

The dominant frequencies of the noise and vibrations data were found by conducting a Fast Fourier Transform (FFT) on the raw data through LabVIEW. The FFT is an algorithm which computes the Discrete Fourier Transform (DFT) in an expedited manner; it is used to convert the collected data from the time domain to the frequency domain [17]. Using the built-in Spectral Analysis virtual instrument (VI) in LabVIEW, a FFT was conducted and the power spectrum of the time domain data was found. Using LabVIEW for the power spectrum measurements was necessary in order to allow for an instantaneous spectral measurement. To further clarify, the data is split into one second long digital bins and each bin contains a certain amount of data samples which

LabVIEW uses to calculate the power spectrum. The moment one bin is filled with all of the data necessary, e.g. 40 thousand samples in the case of the sound measurement, the power spectrum is computed using the samples and the result is then stored on the computer. In this fashion, the power spectrum can be computed without amassing an extremely large amount of data and without encountering issues with signal aliasing. The power spectrum was used in this study because only the frequency values were of interest and not the phase of the signal. For a detailed overview of how the frequency measurements are calculated in LabVIEW, please consult the LabVIEW Measurements Manual [25]. All frequency measurements were collected in units of Hertz (Hz) which represent cycles per second. In order to verify that the frequencies calculated by the LabVIEW spectral measurements VI were correct, a test was conducted by comparing known sound waves ranging from 1 Hz to 20 kHz with the frequency values interpreted by the software. Additionally, the Matlab software package was used on the raw sound and acceleration data in order to calculate the power spectrum and verify the output of LabVIEW. The resulting LabVIEW and Matlab outputs correlated well with one another. Prior to conducting the experiment, all of the data collection equipment was tested for accuracy. The microphone was professionally calibrated and the accuracy of capturing various frequency values was determined by running an acoustical frequency sweep and verifying that the collected data was as expected. The accelerometer was verified by using another calibrated accelerometer to measure a set vibration. The vibration readings from both accelerometers had excellent correlation; thus, the accelerometer used for this study was deemed accurate.

An analysis of variance (ANOVA) was used in determining the significance of train vibrations when compared to the ambient vibrations present within room 103. A single-factor ANOVA was utilized and was formulated in Excel (Microsoft Corporation) based on the theory found in Design and Analysis of Experiments [22]. The statistical work in Excel was verified using a commercial statistical package.

## 2.5 Results and Discussion

### 2.5.1 Results

The highest vibrations in room 103 occurred during the passing of the train. The peak vibrations caused by the passing train were between 0.01 g and 0.025 g and had a frequency range of 12 to 16 Hz. The average ambient vibrations within the LARC were measured to be 0.004 g and the average peak vibrations were 0.015 g. Figures 2.3, 2.4 and 2.5 below display samples of the train vibrations recorded for a typical period of time. Figure 2.3 represents a typical vibration recording for room 103 with mouse cages placed on the flat rack. Trains passed the LARC for one to four minutes, depending on the length of the train. The vibrations produced by the train extend well above the ambient vibrations within the room. The single-factor ANOVA that was conducted on the data indicates that there is a statistical significance between the train and the ambient vibrations. An F-ratio of 58.8 was calculated which correlates to a P-value of 0.0016. Based on a significance level $\alpha$ of 0.05, the null hypothesis was rejected and the treatments were found to be different. The statistical analysis was performed on the data collected for mice on the flat rack.

The results of a typical measurement of a weighted rack without mice, are summarized by Figure 2.4. The vibrations induced by the passing train extend beyond the ambient rack vibrations and are also similar to the train vibrations seen when the rack is loaded with mice. Two peaks occur due to train vibrations in Figure 2.4. The vibrations differ in magnitude and duration. The magnitude of the vibrations is directly proportional to the mass and length of the train. The frequency of the vibrations was not observed to significantly change from train to train.

The vibration measurements taken from the accelerometer in a horizontal position resulted in no apparent peak vibrations. Furthermore, the ambient horizontal vibrations were half the magnitude of the vertical ambient vibrations.

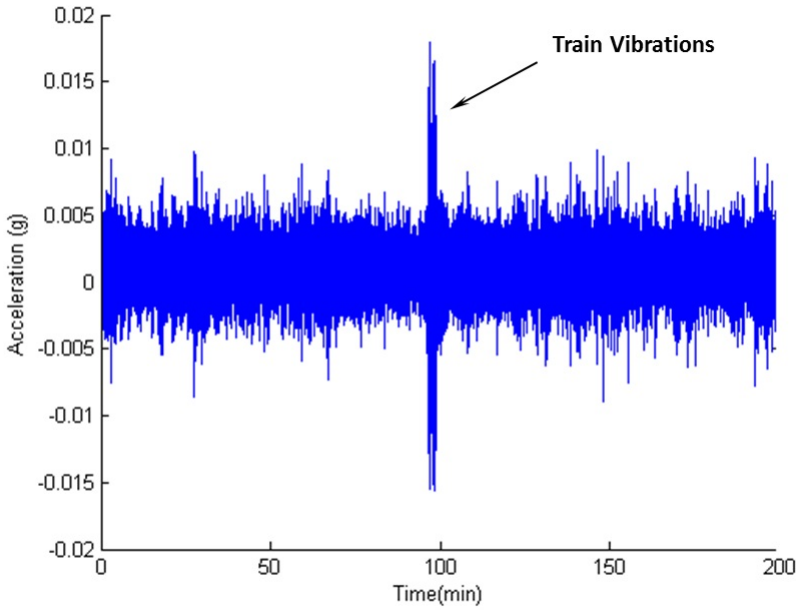


Figure 2.3: Typical vibrations within room 103 with mice on the flat rack

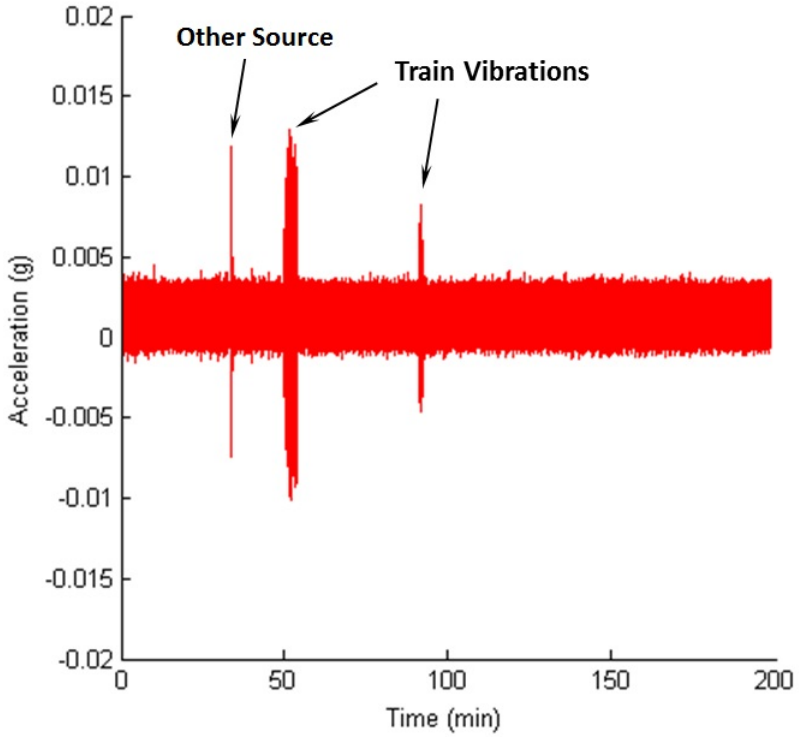


Figure 2.4: Typical vibrations within room 103 without mice on the flat rack but with equivalent weight added

For reference, typical vibrations experienced on a flat rack within the LPSC are shown in Figure 2.5 below. The flat rack within the LPSC had no mice on it and was placed in a room that was not being used. It is important to note that no train vibrations can be observed even though a train passed in the time frame in which the measurements were taken.

The noise recorded in the LARC reached a maximum (average of maximums from all of the recordings) of 108 dB and predominately spanned a frequency range of 1 to 1600 Hz. Figure 2.6 below is a compilation of typical $L_{eq}$ measurements. The sound level fluctuates between 72 and 77 dB with peaks seldom exceeding this range. The largest peak in Figure 2.6 below can be attributed to the signaling horn of a passing train.

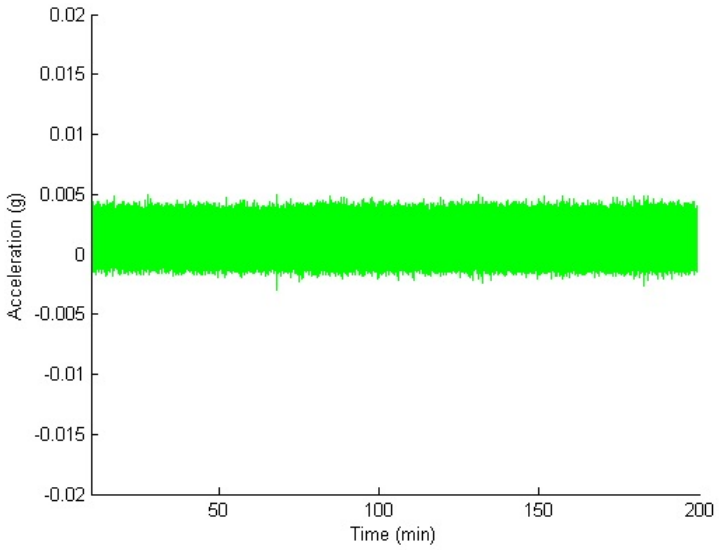


Figure 2.5: Typical acceleration from LPSC room 62

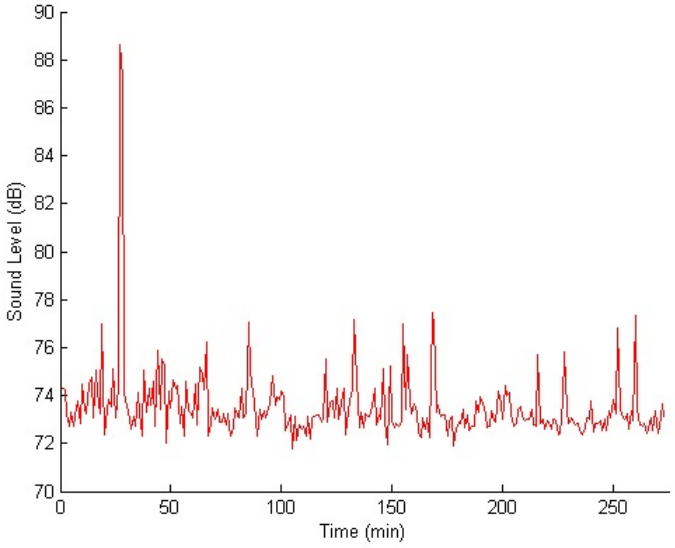


Figure 2.6: Typical Leq of room 103

### 2.5.2 Discussion

The presence of approximately three times larger than ambient vibrations within room 103 of the LARC was confirmed by using a high sensitivity accelerometer. The vibrations within the vivarium were a concern due to the impacts they may have on animal health and experimental outcomes. The recorded vibrations in room 103 are in the frequency range of 12-16 Hz and have magnitudes as high as .025 g. The amplitudes are lower than those of previous investigations on rats, which used amplitudes as high as 2.5 g; however, the frequencies are in a range that has been shown to cause negative effects [2, 35, 36]. Increased adrenal weight, decreased gastric emptying time, elevated plasma corticosterone, and higher brain serotonin levels are noticed in mice and rats exposed to lower frequency vibrations (5-20Hz) [2, 35, 36]. At higher frequencies (90 Hz), the vibrations have been shown to lead to a positive outcome: increased bone formation is observed in mice [39, 40]. The train vibrations in room 103 are unique to the LARC as can be observed by comparing Figure 2.3 with 2.5. No train vibrations are observed in the LPSC, most likely because of the new construction methodologies that were used and the structures distance from the train tracks. The absence of the train vibrations in the LPSC creates a compelling argument to support the hypothesis that vibrations are the cause of reproductive failures within the LARC.

Several important factors were noted during the measurement of the train vibrations: the interaction of technicians and scientists with the racks, the weight and length of the train, and the fluctuation in ambient vibrations. Technicians and investigators play an important role in the proper care of mice and it was observed that, at times, they created large instantaneous vibrational peaks as they handled the cages. These peaks are deemed to not cause a significant impact to the mice because of their extremely short duration; however, these interruptions were addressed and considered during the analysis of the data. The first peak vibration in Figure 2.4, labeled *Other Source*, is an example of a vibration that may have been caused by an event other than the train passing, e.g., technician or investigator handling the cages. The vibration is nearly instantaneous and the video footage does not indicate correlation with a passing train. The weight and length of the train effect the vibrations that advance through the ground. This factor indicates that all train vibrations are unique and that they contribute variety to what the mice experience, which may make it more difficult for the mice to adapt

to the vibrations. The ambient vibrations that occurred in room 103 can mainly be attributed to the activity of the mice within the cages. If the mice have a running wheel or are particularly active during the day, they create larger ambient vibrations. These vibrations may affect the surrounding mice; however, the ambient vibrations tend to stay within a certain range (0.001 to .005 g) and are usually of higher frequency than the train vibrations (30 Hz and over). The mice may adapt to the ambient vibrations more readily and may be aware of the noise and vibrations that their fellow cage mates create.

It is hypothesized that the train vibrations are the cause of poor reproductive success because of their sporadic, relatively high magnitude, low frequency nature. The train vibrations lasted much longer than the vibrations created by the technicians/investigators and were observed to retain higher amplitudes, as compared to the ambient vibrations, throughout the entire passing of the train. The train vibrations may simulate an earthquake more so than the vibrations induced by technicians/investigators and the ambient vibrations. The mice are unable to flee their cages, which may cause them anxiety and an elevation in their stress levels. Vibrations caused by the train also tend to be more irregular than the ambient vibrations and may be an environmental stressor that the mice cannot escape or acclimate to as easily. The trains vibrations occur during the day, a time at which the majority of the mice are asleep, and may cause greater distress in the mice due to disturbances in their nocturnal cycles. The data in the LARC can also be compared to the LPSC, where the train vibrations do not appear to be present.

In the perspective of a human being, the data shows that the vibrations caused by the passing trains are equivalent to a level IV on the Modified Mercalli Intensity Scale (MIS). The MIS is used, alongside the Richter and moment magnitude scales to classify how an earthquake is perceived. According to the MIS scale, vibrations in the IV category can be Felt indoors by many, outdoors by few during the day. Sensation is like a heavy truck striking a building. [11, 38]. The MIS can alternatively be correlated to the Richter scale: it equates approximately to a 4.0 earthquake [11]. As such, mice housed in the LARC may experience the equivalent of a considerable and prolonged earthquake at least three to four times a day.

# Chapter 3: Laboratory Stress Study

## 3.1 Facility and Description

The second part of this study was conducted in the Linus Pauling Science Center (LPSC). The LPSC is located approximately 490 meters away from the railroad tracks which pass the LARC. It is a state-of-the-art facility which opened in 2011. The facility features the latest advances in seismic design and laboratory innovation. Vibration measurements were conducted at the LPSC and the vivarium was deemed to be unaffected by the passing trains.

## 3.2 The Stress Study

The rack inside the test room in the LPSC was instrumented with an accelerometer and initial vibration measurements were taken. It was concluded that no train vibrations existed. Six cages of mice with five mice per cage were used. Three of the cages were male mice and the other three were female, with two cages from each group serving as the experimental animals and the other cage as the control. The animals were moved into a designated room within the LPSC one week prior to the study. Starting four days before the study, the tails of all the animals were marked and the animals were subjected to a cage transfer routine. The routine consisted of individually moving the animals, twice a day, into empty cages using a short piece of PVC pipe (included in each cage as enrichment). Each animal remained in a separate cage for three minutes before they were returned to the main, group cage from which they were originally moved. The routine was used to acclimate the animals to handling in a specific manner and to individual housing for short periods of time. The concept of using a PVC pipe arose from a preliminary study in which the animals were moved by their tails. It was hypothesized that this form of handling could produce stress in the animals, which may skew the test results.

The day of the study, two cages of five males and two cages of five females were

Table 3.1: Summary fecal collection and vibrations times

| **Activity** | **Time of Day** |
|---|---|
| Vibration, Fecal Collection | 12pm |
| Vibration | 1:30pm |
| Vibration, Fecal Collection | 2:30pm |
| Fecal Collection | 5pm |
| Fecal Collection | 7:30pm |
| Fecal Collection | 9:30pm |
| Fecal Collection | 11:30pm |

vibrated in their home cages using an electromagnetic shaker. Each cage was vibrated individually. The induced vibration had a frequency of 14 Hz and a maximum amplitude of approximately .025 g, both values are characteristic of the vibrations recorded in the LARC during the passing of a typical train. The cages were vibrated at about 12:00pm, 1:30pm, and 2:30pm with each vibration episode lasting four minutes. The times of vibration were selected based on the times at which the train typically passes the LARC each day. One cage of males and one of females were used as the control group and were set on the vibration platform but were not vibrated. Fecal sample collection began after the first set of vibrations. Table 3.1 outlines the approximate times that fecal sample collection began and when the cages were vibrated.

The room lights shut-off at 6 pm; after which, the red, built-in, ceiling lights were used during collections in the dark. The mice were, by meticulously maintaining their separation from other test groups, moved into individual, clean cages lined with a paper towel. The investigators waited until each animal excreted three fecal samples and then moved the animal back to its respective group cage. All fecal samples were collected with tweezers, placed in individually labeled 2 mL Corning tubes, put immediately on dry ice, and moved into a minus 30 degree Celsius freezer for storage. The samples were dried and extracted at OSU; the processed samples were then sent to the University of Veterinary Medicine in Vienna, Austria for a fecal corticosterone metabolite (FCM) analysis.

## 3.3 Electromagnetic Shaker

An electromagnetic shaker was selected as the method with which to induce vibrations because of its ability to produce high frequency movements; however, due to the exorbitant costs of commercial electromagnetic shakers, an alternative method was developed to produce vibrations in a controlled manner. An electromagnetic shaker is comprised of an electromagnet situated between a permanent magnet. By changing the direction of the electrical current flowing through the electromagnet, the polarity of the magnet can be manipulated. By manipulating the polarity of the electromagnet, it will either be repelled from or attracted to the permanent magnet. The concept of electromagnetism is readily applied to loudspeakers, which function in the same way. A subwoofer, a loudspeakers designed for low frequency sounds, was a good candidate for creating an electromagnetic shaking system. Subwoofers are typically larger in size as compared to other speakers, this was important because a bigger surface area was needed for the final vibration system. A 200 Watt Audiovox Rampage subwoofer and a new Russound X75 2-channel dual source amplifier were purchased. The amount of power supplied to the subwoofer was regulated by the amplifier. An airtight housing was designed and constructed for the subwoofer. The housing was made of medium-density fiberboard (MDF) and contains wires connecting the subwoofer to the amplifier. The housing was constructed to be as airtight as possible and thus allowed for the entrapped air to apply pressure to the subwoofer as it oscillated. The additional air pressure allowed for a flat frequency response, which meant that the subwoofer was more likely to output the frequency that was being input into the speaker system. Two diagrams of the system are displayed in Figure 3.1.

The vibration system was constructed with a MDF housing, which was manufactured by combining fine wood fibers mixed with glue and heat pressing the two compounds together. The MDF was chosen due to its lack of voids and relatively high density, both which help contain the vibrations that resonant from the device. The subwoofer was situated directly in the center of the housing and a vibration platform was adhered to the cone. The platform was designed to support one cage at a time, a constraint which arose from the strength of the cone material and the driving force capabilities of the subwoofer. The wiring connecting the subwoofer to the outside remainder of the system was routed through a speaker terminal. The speaker terminal accepts banana

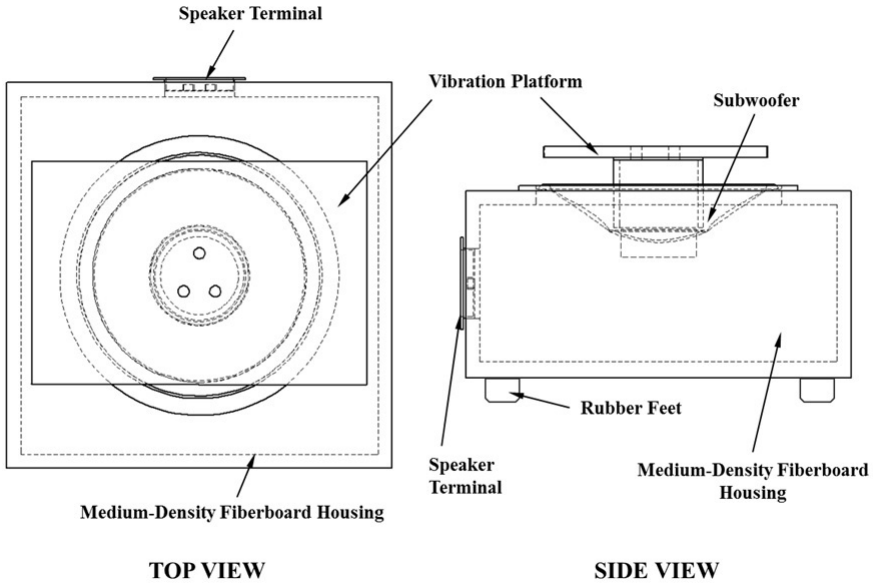


Figure 3.1: Top and side view of the electromagnetic shaker

plug connectors, which allow for an easy connection of the amplifier to the subwoofer. Lastly, rubber feet were installed to limit the transfer of vibrations to the surrounding environment and to level the system. Aside from the physical aspects of the system, the vibration signal had to be generated using a computer and the amplifier.

The Matlab software was used to create a 14 Hz sinusoidal waveform. The vibration produced by the train is not modeled perfectly by a sine wave; however, a sine wave acts as a relative representation of the induced motion during the passing of the train. Furthermore, harmonic motion can be more readily produced if future studies are to be conducted and the results can be more easily compared to the outcomes of this study. Equation 3.1 was used to model the train vibrations.

$$y(t) = A * sin(\omega * t + \phi) \tag{3.1}$$

In Equation 3.1, $A$ is the amplitude of the vibration, $\omega$ is the frequency, $t$ is time, and $\phi$ is the phase angle. The Matlab program was used to generate the sine wave in Equation 3.1 with an amplitude of one unit, a frequency of 14 Hz and a zero degree phase

angle. The sine wave was converted into a sound file and was transferred through the audio port of the computer to the amplifier. The amplitude of the sine wave was set by adjusting the volume of the amplifier: increased volume yielded increased amplitude. The entire vibration system was calibrated to the correct setting by placing the instrumented measuring cage on top of the vibration device and measuring the vibrations produced by running the device. The amplitude was adjusted until 0.025 g was reached. The frequency measured was exactly the frequency that was input, 14 Hz; therefore, the device performed as designed.

## 3.4 Mice

The animals were housed in an environment of 22 degrees Celsius with simulated day and night times by 12:12 hour dark-light cycle. After pre-weaning, five animals were maintained per cage on standard bedding in ventilated racks. The diets of the animals were as follows: for breeding animals - pelleted (2919, Harlan) breeding diet; for weanlings and non-breeding male mice - standard pellet diet (5053, Purina). Water pouches (Lab Products HydroPac) were given ad libitum. All of mice used in this part of the study were standard laboratory mice (ICR type, Charles River Laboratories) and were born in the LPSC. Husbandry, lighting conditions, and health status are as per suggestions of Guide for the Care and Use of Laboratory Animals [8] . Mice were moved onto a flat rack in the room where vibration exposure would occur one week prior to the start of experiments for acclimation. The mice were 15 weeks old at the time of vibration exposure and measurements.

## 3.5 Data Analysis and Statistical Methods

Unlike Part I, the data analysis for Part II was mainly focused on the FCM levels of the mice rather than the vibration measurements. Vibration measurements were only conducted to calibrate the vibration device and to measure the vibrations in the building prior to conducting the study. The FCM results obtained from the laboratory in Austria, were analyzed using a multi-factor ANOVA with 90 percent and 95 percent confidence intervals. The ANOVA were used to determine if significance existed between the control and experimental groups. Plots were generated for all of the results in order to visually

analyze the data and draw conclusions.

## 3.6 Results and Discussion

### 3.6.1 Results

Figures 3.2 and 3.3 represent averages of the FCM levels of the various test groups at different times of the day. For example, three curves are given in Figure 3.2 , the Females 1 and 2 curves represent the average FCM levels of all the mice within either female cage 1 or cage 2. In the same manner, the Female-Control curve in Figure 3.2 represents the averages within the female mice control cage. Figure 3.3 for the male mice group follows the same labeling scheme as that used in the figure for the females. In Figures 3.2 through 3.5, the black diamonds in the lower left-hand corner indicate the times at which vibrations were induced with the electromagnetic shaker. The solid, vertical, black line is the transition from the day to night light cycle.

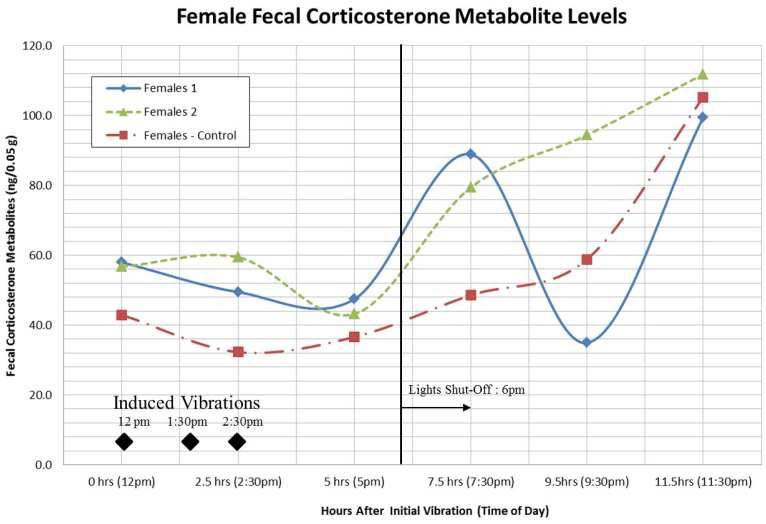


Figure 3.2: Plot of averaged FCM levels in the female mice group

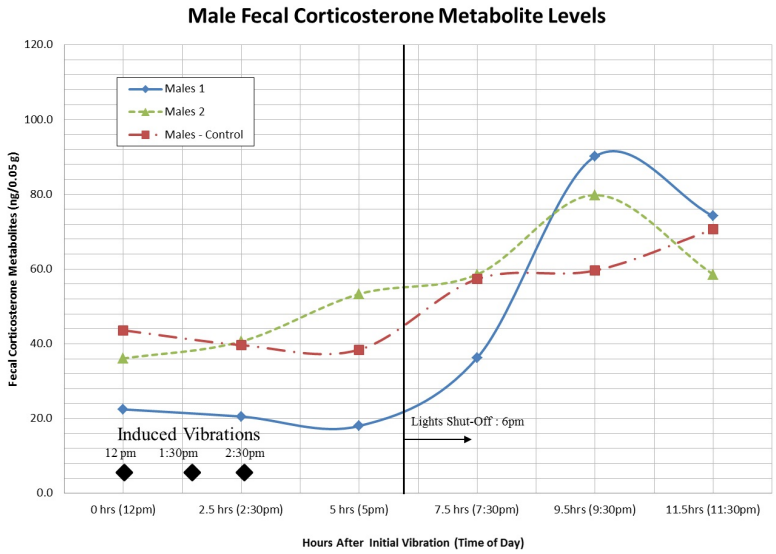


Figure 3.3: Plot of averaged FCM levels in the male mice group

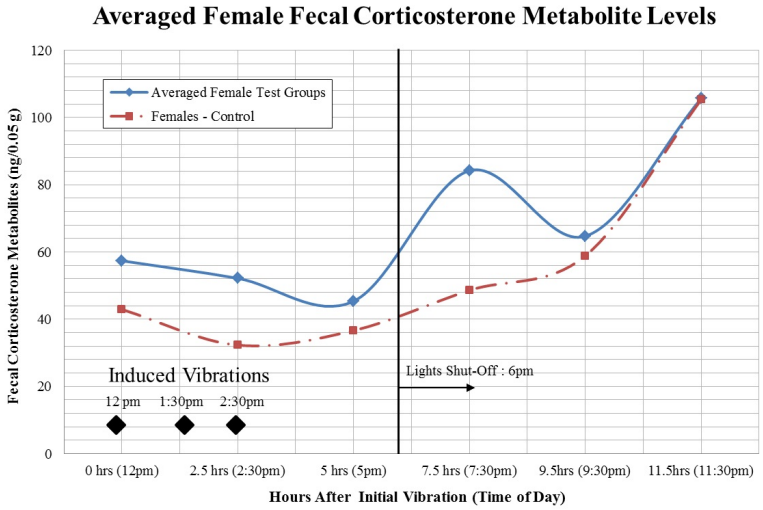


Figure 3.4: Plot of combined average FCM levels in the female mice group

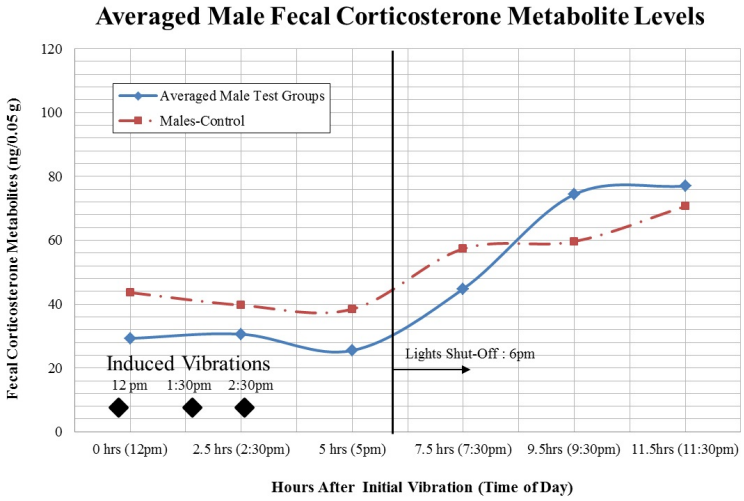


Figure 3.5: Plot of combined average FCM levels in the male mice group

Figures 3.4 and 3.5 are nearly the same as Figures 3.2 and 3.3, except that the test curves are averaged together in order to compare the combined result to the control groups. For example, the Females 1 and 2 curves in Figure 3.2 are averaged together to produce the combined *Averaged Female Test Groups* curve.

A single factor ANOVA was used to determine the statistical significance between the different groups, e.g., female group 1, 2 and control. The ANOVA was conducted within each period of time so as to eliminate consideration of the time of day. Within a 90 percent confidence interval, the stress levels of female groups 1 and 2 were deemed to be significantly different from one another 7.5 hours after the first vibration was induced. Within a 95 percent confidence interval, female group 1 was significantly different as compared to female group 2; however, only one female test group was significantly different when compared to the control. The male groups had a statistical outcome that differed from that of the females. When compared to the male control group, the male group 1 was significantly different, within a 95 percent confidence interval, throughout the majority of the study. 9.5 hours after the first vibration was induced, the males in group 1 were deemed to be significantly different when compared to the controls and to male group 2. Male group 2 tended to parallel the control group far more than it paralleled the first male test group; this conclusion can be visualized in Figure 3.3 above.

### 3.6.2 Discussion

Part II of this study investigated the effect train vibrations have on the FCM levels of female and male mice in order to obtain a quantitative measurement of how the vibrations impact the mice. The female and male test groups, as seen in Figures 10 through 13 exhibit sporadic behavior in the region between 5 pm and 11:30 pm. The behavior is judged to be sporadic based upon a comparison with the control groups which do not display any large, sudden fluctuations. To focus on the females firstly, the two test groups display a similar peaking behavior at 7:30 pm but they differ drastically at 9:30 pm. It is hypothesized that the peak seen at 7:30 pm is due to the vibrations induced by the electromagnetic shaker. The analysis of variance further confirms that there is a significant difference between the female test groups and the female control group. It is has been documented that an event causing fluctuations in stress levels within mice will manifest into fluctuations in their FCM levels between 6 and 9 hours after the event has occurred [16, 37]. The extreme decrease at 9:30 pm in FCM levels of female group 1 in Figure 10 is difficult to explain. The analysis of variance suggests that the female test groups are significantly different when compared to one another at 9:30pm, though no significant difference exists when the test groups are individually compared to the control group. It is also important to note that both female test groups have higher stress levels at 12:30 pm, as compared to the control group. The increased stress levels in the beginning of the study are somewhat mysterious; however, the fecal samples were collected immediately after the first vibration episode. Nevertheless, the resulting stress levels of all the female groups, including the control group, were relatively similar at 5 pm. Fluctuations in stress, whether high or low in magnitude, can be detrimental to a study in which stress levels are being used to analyze the effect of a substance or a particular situation. The fluctuations will, undoubtedly, alter the final results. Elevated levels of anxiety and stress may also promote the increased growth of cancerous cells and completely skew an experiment in which cancer is the key disease being studied [9]. The female groups are of particular importance because the female mice are the ones that give birth and primarily care for the offspring. If the females are greatly distressed, they may have poor reproductive success and may hurt or cannibalize their young shortly after birth. The fluctuating corticosterone levels have lead the authors to believe that the females are negatively impacted by train-like vibrations and mice at the

LARC may experience poor reproductive success due to the passing trains. The male test and control groups are also of importance, though they seemed less affected by the induced vibrations.

The male test and control groups exhibited, in general, slightly lower FCM levels than the female groups. Both male test groups are graphically seen to deviate from the male controls and peak at 9:30 pm. When compared by analysis of variance methods, a significant difference existed between male group 1 and the male control group for nearly the entire testing period; however, no such difference was prevalent when male group 2 was compared to the control group. Male test group 2 deviated less from the control group as compared to male group 1, male group 2 also had lower fluctuations on average. The lower stress response from the males may possibly be attributed to the gender. The female estrous cycle may play a role in the difference between the male and female responses. The male mice test groups, unlike the female test groups, have either similar or lower corticosterone levels than the control group. Aside from specific differences between genders, generalities exist amongst both the female and male groups. For both female and male mice, an elevation in corticosterone is seen after 5:30 pm, just before the lights were turned off. At 11:30 pm, the levels of all of the groups start to coincide and once again track together.

# Chapter 4: Mitigation of Train Vibrations

Designing and creating a vibration isolation solution is the final part of this study. The basic theory of vibration isolation, the steps taken to find suitable isolators, and verification of the new system's performance are all topics covered in this chapter. All of the data collected in the previous portions of this study contributed to a more effective design. The train vibrations were characterized as perceived by a mouse (in a cage and on a wire rack) and their effects were studied in a well regulated setting. The train was determined to create vibrations well above ambient and to bring about fluctuations in the FCM levels of female and male mice. The fluctuations in FCM levels can be problematic in any study using mice because of their effect on cancer growth, mouse behavior, and overall mouse physiology; therefore, the goal of this portion of the study is to decrease the amplitudes of the train vibrations to levels which are equivalent to the ambient vibrations in the room 103.

## 4.1 Basic Theory of Vibration Isolation with Applications to this Study

Vibration isolation problems are often complex phenomena which can be represented, for the purpose of practical engineering solutions, using simplified models. The models used to represent vibrating systems are based on mathematics and observation, the combination of both yielding the most satisfactory results. In order to select the possible model, an understanding of the theory of vibration isolation is necessary.

Establishing proper models for vibration systems is based upon determining the exact problem to be solved and formulating the necessary assumptions that will allow for ease in solution derivation yet represent the fundamental physics present in the system. Vibration problems can either be vibration isolation or shock isolation problems. Vibration isolation problems are usually ones in which a harmonic, continuous input is affecting the system in question. Such inputs as a passing train, reciprocating machinery, and heating/cooling units within buildings can all cause harmonic loading of a system.

Shock isolation problems differ from vibration problems in that the loading of the system occurs for a short duration, most often for a time span less than one natural time period of the system [30]. The equations used to model the system differ for vibration isolation and shock isolation problems; therefore, it is critical that the inputs present are properly characterized.

The vibration problem encountered in this study is that of an assumed harmonic input that has a duration of several minutes, thus a vibration isolation model is considered. Most vibration isolation problems consist of a resilient member (also referred to as a stiffness element) and a damping element, or damper for short. The resilient member stores potential energy while the damping element dissipates energy [28, 30]. The resilient member usually itself has very low damping characteristics and is best exemplified by metal springs. The damper dissipates energy in the form of heat through the phenomena of hysteresis [4]. Hysteresis occurs due to internal friction within the material, which is caused by material planes that slip or slide as the material changes shape [30]. The resilient member is responsible for changing the overall characteristics of a system because the natural frequency is directly dependent on the stiffness of the element. The natural frequency is the frequency at which, if initially disturbed, an elastic body will oscillate at in the absence of a driving force [30]. The natural frequency for a single-degree-of-freedom (SDOF) system is represented by Equation 4.1.

$$\omega = \sqrt{\frac{k_{eq}}{m_{eq}}} \tag{4.1}$$

In Equation 4.1, $k_{eq}$ is the equivalent stiffness of the system and $m_{eq}$ is the equivalent mass. The equivalent stiffness and mass are representative of all stiffness and mass elements within the system. A system may be comprised of several stiffness and mass elements that can be combined into single quantities. For example, the stiffness of a SDOF system can be comprised of several stiffness elements either in series or in parallel. Stiffness elements in series can be combined by the relationship $1/k_{eq} = 1/k_1 + 1/k_2 + ... + 1/k_n$ while stiffness elements in parallel are combined by direct addition as in $k_{eq} = k_1 + k_2 + ... + k_n$. An example of system simplification is given in Figure 4.1.

The system in Figure 4.1 displays how a system with three spring or stiffness elements and two rigidly connected masses can be transformed into an equivalent mass-spring system. The $M_{eq}$ is equal to $M1 + M2$ and the $k_{eq}$ is comprised of $k_1 + k_1 + k_1$, as per

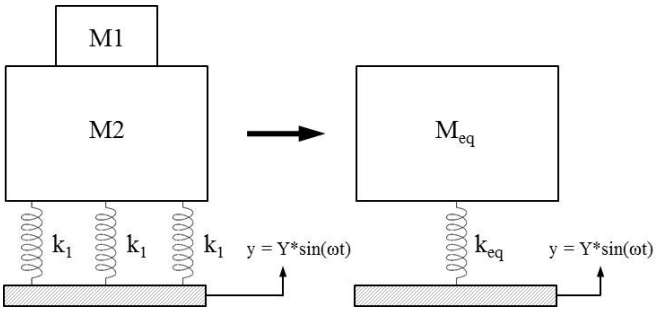


Figure 4.1: Example of equivalent mass-spring system

the parallel stiffness element relationship. The ability to combine stiffness elements and lump masses is important in this study because the rack is comprised of several stiffness elements and masses on every shelf.

For a simplified model, damping can be ignored, especially if an isolation system is used which has low damping characteristics. For many practical applications, a SDOF system model is assumed [15]. The SDOF model is one in which the system to be isolated is represented by a single point mass. A representation of the SDOF system is the right-hand image in Figure 4.1. It is important to note that the base, or the element below the spring, has a displacement function $y = Y sin(\omega t)$ associated with it. The displacement function indicates that the system is undergoing base excitation. The base excitation assumption is used in this model because the ground will displace vertically as the train vibrations move through it. The spring element will be the first to encounter the ground fluctuations and will consequently transfer them to the mass above it. Problems in which the excitation energy of the system travels through a spring, and indirectly affects the mass, are known as base excitation problems. The simple base excitation problem can be represented by Equation 4.2 [30, 15].

$$|\frac{X}{Y}| = \frac{k}{k - m\omega^2} \tag{4.2}$$

In Equation 4.2, $k$ is the stiffness of the system $m$ is the mass and $\omega$ is the frequency of excitation. The amplitude of the displacement response is $X$ and the amplitude of the displacement forcing is $Y$. Therefore, it can be observed that the base excitation response of the system can be represented by the amplitudes of the displacements. Equation 4.2 is referred to as the displacement transmissibility. Plotting the displacement transmissi-

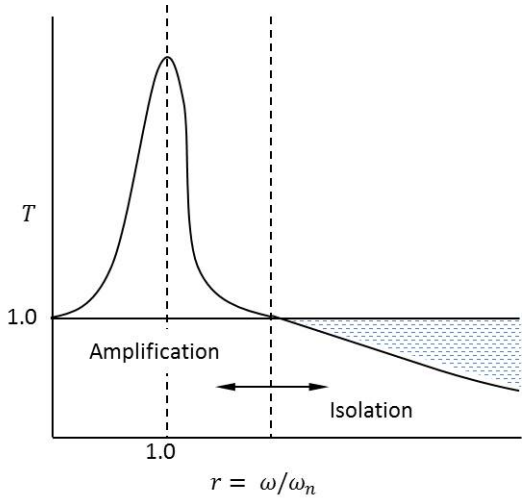


Figure 4.2: Sample transmissibility plot

bility against the frequency ratio $r = \omega/\omega_n$ results in a transmissibility plot. A sample transmissibility plot is shown in Figure 4.2.

The section of the transmissibility plot marked as the isolation region will yield a transmissibility less than 1, which means that the displacement of the mass will be less than the displacement of the ground below the stiffness element. The mass will be isolated from the forcing. Whether the forcing/displacement in a system is amplified or isolated is a function of the natural frequency of the system and the frequency of the forcing function. The frequency ratio is the ratio of the forcing frequency over the natural frequency; hence, by manipulating the stiffness and mass of the system, the frequency ratio can be raised and the mass can be isolated. The isolator design in this study will be based on the premise of the transmissibility plot and an isolation system will be selected that gives the greatest isolation against the train vibrations at the lowest possible cost.

The transmissibility plot can be used to select a vibration isolation solution; however, the selection must narrowed down from all of the available isolator options. Isolators can be categorized as either passive systems or active. Active systems have the ability to sense incoming vibrations, by means of an accelerometer or other devices, and adjust accordingly to the input [30]. An example of an active isolator is a pneumatic cylinder that inflates or deflates based on the sensed vibration, thereby providing real-time changes

in the vibration characteristics of the system. Active isolators usually offer the most optimized protection from unwanted vibration; however, they are also more expensive to implement and operate as compared to passive isolators. Passive isolators do not adjust to the vibration by means of active sensing units (accelerometers), instead they have set characteristics. The properties of passive isolators may vary, however, depending on the frequency and load applied to them due to non-linear material behavior. Examples of passive isolators include elastomeric mounts/pads, pneumatic springs with no active sensing, and metal springs [28]. Passive isolators are used in many applications where a cost effective solution is desired and where extremely precise mitigation of vibrations is not required.

## 4.2 System Characterization

In order to properly determine an adequate solution for the vibration problem, the characteristics of the existing system had to be determined. System characteristics included the response of the flat rack to the vibration of the train, the train vibrations as recorded on the ground near the rack, the mass of the rack, and approximate stiffness of the rack. In order to determine all of the system parameters, accelerometer and stiffness measurements were completed and the mass of the system was calculated.

The response of the rack system to ground vibrations in room 103 was recorded in the initial phases, as outlined in the results section of Chapter 2. An average acceleration amplitude of 0.015 g was measured for the response at an approximate frequency of 12-16 Hz, the main frequency being 14 Hz. The ambient vibration in room 103 were recorded to be 0.004 g on average.

The train vibrations on the ground near the rack were measured in order to determine the forcing amplitude and frequency of the train. The forcing acceleration amplitude is required for an experimental calculation of the transmissibility while the frequency is necessary in determining the theoretical transmissibility using a measured stiffness value, a calculated mass, and Equation 4.2. The forcing of the train was determined by using an accelerometer to measure the ground vibrations in the location of room 103 where a flat rack was normally located. The accelerometer was secured to the ground using beeswax and the passing of the train was verified with video footage. Vibration measurements were conducted for three days for five hours per day. The five hour collection period

allowed for the passing of two to three trains, which were enough to characterize the ground vibrations. Once the vibrations were collected, an FFT was performed on the data in order to determine the frequency of the vibrations and the maximum amplitudes. A sinusoidal forcing function was assumed in order to simplify the calculations and due to the periodic motion of the train (the train wheels create for periodicity as the train moves across the tracks). The measured amplitude of vibrations during the passing of the train was approximately .01 g at a frequency of 18 Hz.

The mass of the flat rack was calculated by using manufacturer mass values for the various components of the rack. The rack was not directly weighed due to a lack of equipment for weighing an object of its size and shape. The approximate rack dimensions are: 1.9 m high, .46 m wide, and 1.8 m long. The rack includes five shelves and four vertical rods weighing 9.1 kg and 1.8 kg, respectively. The total combined self-weight of the rack, excluding the casters, is 52.7 kg. The caster weight is neglected because the casters are assumed to be massless stiffness elements, this will be discussed in the section that follows. Two sets of additional weight values are assumed for the rack: a weight value to account for a medium mouse cage loading on the rack and a weight value for a high mouse cage loading. The medium value cage load represents a averagely loaded rack containing 20 mouse cages, with the mass of each cage being approximately 2 kg. The total medium cage load will thus be 40 kg. The high cage load represents a fully loaded rack which contains 9 cages per shelf with the highest shelf neglected due to its height and difficulty it poses for the technicians in terms of accessibility. The total high load values comes out to be 72 kg. The mass of each cage is accounted for by the contents within: food supplies, water, bedding, and the mice themselves. The total masses of the racks, including self-weight and the weight of the mouse cages are as follows: medium load - 93 kg, high load - 125 kg. The loads will serve as a range of masses that the rack will be loaded to. The mass of the rack without mice is not considered here because no animals will be impacted by the vibrations of the rack if there are no animals present on the rack.

Using the SDOF model simplification, the rack was assumed to act as a point mass while the casters provided the entire system stiffness. The stiffness of the casters was determined by using an Instron mechanical testing system. The testing system was used to generate a load versus displacement curve for a single caster. The slope of the curve was taken to be the stiffness of the individual casters. The resulting plot from the

mechanical testing is shown Figure 4.3.

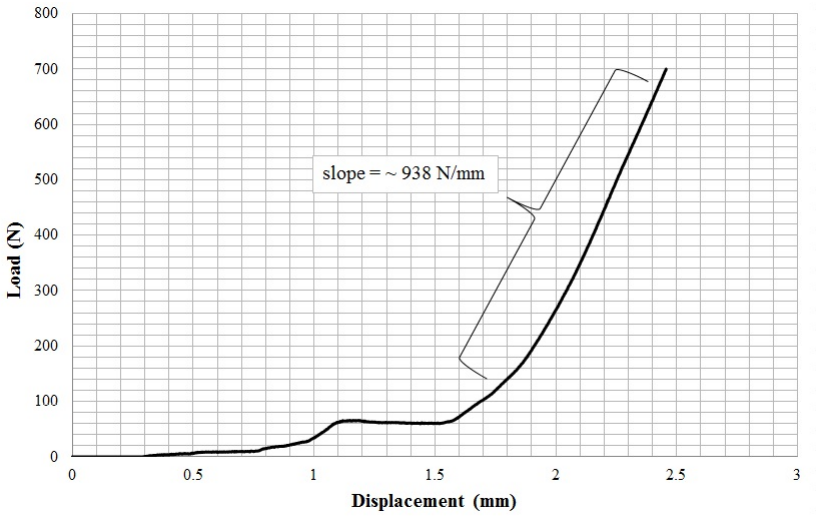


Figure 4.3: Sample transmissibility plot

In Figure 4.3 the behavior of the caster changes at different loads until about 130 N is reached, at which time the load versus displacement curve remains linear. The linear portion of the curve was taken as the stiffness of the system because a load of at 130 N or greater is always present on each caster due to the self-weight of the rack. The slope of the linear portion of the load versus displacement curve is approximately 938 N/mm.

With the necessary system parameters determined, the isolation design for the system could commence. A summary of all the original rack characteristics is given in Table 4.1.

Table 4.1: Summary of original rack characteristics

| **Parameter** | **Value** |
|---|---|
| Mass (kg) | Medium Load:92.7, High Load:125 |
| Forcing Frequency (Hz) | 18 Hz |
| Forcing Amplitude (g) | 0.01 |
| Response Frequency (Hz) | 14 Hz |
| Response Amplitude (g) | 0.015 |
| Response Ambient Amplitude (g) | 0.004 |
| Caster Stiffness (N/mm) | 938 |

## 4.3 Isolator Design

The isolator design consists of determining a way to isolate the rack from the train vibrations which travel through the ground beneath it. The first step in the isolator design is determination of a goal. The goal in the case of this study was to isolate the train vibrations so that their amplitude matches that of the ambient vibrations. In order to meet the goal, the following steps were taken:

1. A simplified system model was assumed and verified
2. A range of stiffness values was selected based on transmissibility plots created via the simplified model
3. Isolators available on the market were compared in order to find the best possible solution

The ambient vibrations within room 103 were measured to be 0.004 g on average; therefore, a transmissibility value can be calculated assuming that the maximum value of the train vibrations is the value of the ambient vibrations. With all of the parameters in place transmissibility plots were created based on Equation 4.1 and the assumed natural frequencies of the system based on the medium load mass and the high load mass.

### 4.3.1 Assuming a Simplified Model and the Transmissibility Plot

In order to design an adequate system, yet still maintain simplicity in the design, the basic base excitation model outlined in the vibration theory section above was assumed for the mouse rack. The model is a single-degree-of-freedom (SDOF) system with the main body of the rack being a point mass and the casters being stiffness elements. Damping undoubtedly exists in the system but was be ignored for the sake of simplicity. However, even though damping is ignored, the worst-case scenario is considered because damping will only aid in decreasing peak loads seen in the system. Any damping that results in the system, designed in or otherwise, will have a positive effect (cautionary note: too much damping in a system may actually impede the isolation characteristics; however, such large damping should not be present, especially if metal spring or pneumatic isolators are used). The simplified model follows Equation 4.2 and was verified via experimentation. It was important to verify the model in order to determine its viability in representing changes in the system. Verification consisted of comparing the transmissibility values of the experimental maximum rack displacement and maximum ground displacement with the modeled transmissibility. The experimental maximum displacements were determined by assuming a sinusoidal function for the train vibrations as measured in the mouse cage on the rack and as measured on the ground (note: the experimental measurements were taken with a rack having a medium load value). For the acceleration response function, a dominate frequency of 14 Hz (87.9 rad/sec) was assumed with a vibration amplitude of 0.015 g. For the acceleration function of the ground vibrations, a frequency of 18 Hz (113 rad/sec) with an amplitude of 0.01 g was used. The data collected on the rack and on the ground is in terms of acceleration; however, the data is desired in terms of displacements in order to calculate a displacement transmissibility. Sinusoidal functions were assumed; therefore, the accelerations can be represented by Equation 4.3 [30].

$$a = -\omega^2 A \cos(\omega t - \phi) \tag{4.3}$$

In Equation 4.3, $\omega$ is the frequency of the vibrations, $A$ is the maximum displacement, $t$ is time, and $\phi$ is a phase angle, which can be interpreted as the angle between the origin and the first peak [30]. The maximum displacement is desired for the rack vibrations and the ground vibrations; thus, the maximum displacements can be assumed by having

the cosine term be at a maximum, i.e. $\cos(\omega t - \phi) = 1$, and using the respective rack and ground frequency values. The resulting maximum displacements for the rack and ground are 0.0190 mm and 0.0077 mm, respectively. The rack displacement was divided by the ground displacement, which resulted in an experimental transmissibility of 2.47. It is important to note that if the frequency of the rack and the ground vibrations, during the passing of the train, were the same, the displacement transmissibility would be the same as the acceleration transmissibility and would result in a value of 1.5. The experimental transmissibility was then compared to the analytical transmissibility.

Analytical transmissibility values were found via Equation 4.2 using the forcing frequency of 18 Hz (113 rad/s), the rack masses of 92.7 kg (medium load) and 125 kg (high load), and the equivalent caster stiffness value of 3752 KN/m (as obtained by combining the stiffness values of four casters in parallel). The resulting transmissibility values are 1.46 for the medium load and 1.74 for the high load. Figure 4.4 is a graphical representation of the transmissibility curve, which is the same for a medium or high rack load because the transmissibility is plotted against the frequency ratio which also changes in proportion to the mass.

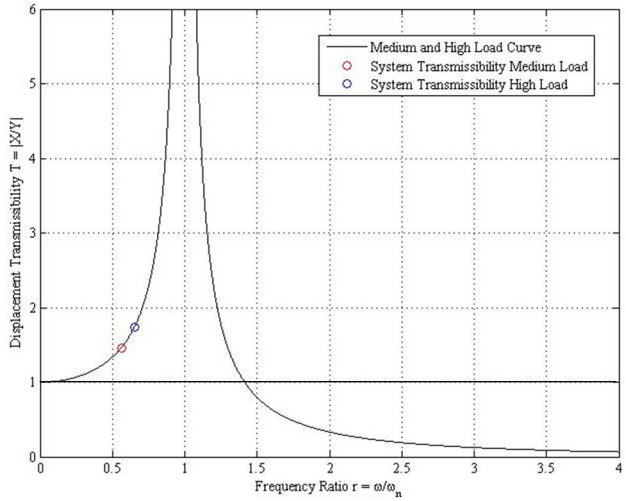


Figure 4.4: Transmissibility curves for medium and high load values

Figure 4.4 contains two point which represent the transmissibility values for the orig-

inal system with the medium and high load values.It can be seen that,up to a point, the vibrations are amplified as the load increases. The analytically calculated transmissibility values for a medium loaded rack were compared to the experimental transmissibility values in order to determine the adequacy of Equation 4.2 in representing the system. The analytical transmissibility value was 1.46 while the experimentally found value is 2.47, an approximately 52 percent difference. If the acceleration transmissibility is used rather than the displacement transmissibility, this being the same as the response vibration frequency being equal to the ground vibration frequency, then a value of 1.5 results. The acceleration transmissibility is almost exactly equal to the analytically computed transmissibility. With the experimental transmissibility and analytical transmissibility being relatively similar, the simplified model was deemed to be satisfactory.

The transmissibility curve in Figure 4.4 was used, along with an iterative procedure to select the necessary system stiffness to provide for adequate vibration isolation, the iterations were conducted in Matlab with the code found in Appendix A. Equation 4.2 can be used to iterate to a stiffness value for the system which results in a displacement transmissibility equal to that of the ambient vibrations. The maximum displacement amplitude for the ambient response vibrations was calculated with Equation 4.3 and is 0.0051 mm and the required transmissibility is 0.66. The back calculated equivalent stiffness values for a medium loaded and high loaded rack are 470 and 634 KN/m, respectively. The lower stiffness value is the limiting parameter because if the rack is isolated when medium loaded, it will be isolated when it is heavily loaded. The value of 470 KN/m was used to find a set of isolators that, when combined, can minimize the train vibrations.

### 4.3.2 Isolator Device Selection and Design

Once the required equivalent stiffness of the system was found and the major system parameters were characterized, a suitable isolation solution was designed. The design process can be summarized by Figure 4.5.

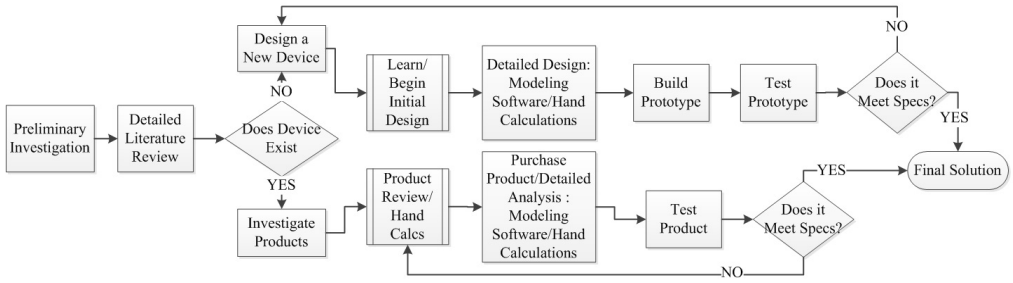


Figure 4.5: Flowchart outlining the selection/design process of the vibration mitigating device

Initial research was done in order to determine the availability of devices on the market and it was determined that enough existing isolator exist which can be readily applied to the current vibration mitigation problem. The vibration isolation options were narrowed down based on a set of required and optional criteria. First and foremost, the retro-fitted rack needs to be isolated from the train vibrations. The isolation requirement was determined in subsection 4.3.1. The vibration isolation system has to also be able to withstand temperatures of up to 160 degrees Fahrenheit as it is cleaned periodically in a specialized washer. The rack washer uses water and cleaning agents in order to remove bacteria from the rack; therefore, the selected isolating system has to be able to withstand a wet environment and light chemical attack. Additionally, the selected isolator system has to be able to provide stability/support to the rack structure vertically and laterally. The isolation system has to be easy to maintain and use by technicians in the LARC. Ideally, the system will require no adjusting; however, over time, the system may need to be changed due to wear of the isolation components or a variation of the forcing vibrations. In regards to cost, the overall system should be under 200 dollars in cost, as dictated by the limited budget available through the LARC. Furthermore, if a vibration isolation system is less costly, the LARC will be able to implement the solution on more of their racks. It is desirable for the isolation system to have a small amount of damping, though it is not calculated within the design, and to also have a certain level of stiffness adjustability. The damping within the isolator will provide for some protection against excessive vibration amplitudes should the system be exposed to its resonant frequency. The level of adjustability is difficult to quantify due to the limits of each material or device; however, the more adjustability a system has, the more

robust the solution would be because system characteristics can tailored to the current circumstances more readily. Table 4.2 summarized all of the design requirements.

Table 4.2: Comparison of criteria for isolator selection

| | **Elastomers** | **Metal Springs** | **Pneumatic Springs** | **Helical Cable** |
|---|---|---|---|---|
| **Reduction Capability** | X | X | X | X |
| **Temperature Range** | X | X | X | X |
| **Easy of Use** | X | X | X | X |
| **Cost** | X | X | X | X |
| **Adjustability (optional)** | | | X | |
| **Inclusion of Damping (optional)** | X | | X | X |

In Table 4.2, only passive isolation options were considered due to cost requirements and ease of implementation/use. Active isolation options cost upwards of 1000 dollars and have more components that will requires maintenance/calibration. The $X$s in Table 4.2 indicate whether a certain criteria has been met. Some criteria were required and others were simply desired (the criteria marked "optional"). Based on the simple comparison table, the pneumatic springs appeared to be the best option. However, all of the options were investigated closely in order to determine the most suitable solution. Each solution was considered as a device to be implemented between the caster and the rack. In this fashion, a general caster assembly could be created and different isolation devices could be substituted readily until the most ideal solution is found.

The general caster assembly consists of a new set of casters which have a four bolt attachment configuration. This enables the casters to be attached and removed easily as opposed to the original stem casters which have a locking ring and require large amounts of impact force to dislodge them from their set location. The new set of casters also is nearly three times stiffer than the original set with a value of 2707 KN/m. The stiffness of the new casters was determined by using the Instron mechanical testing system to generate a load versus displacement curve. The curve is displayed in Figure 4.6.

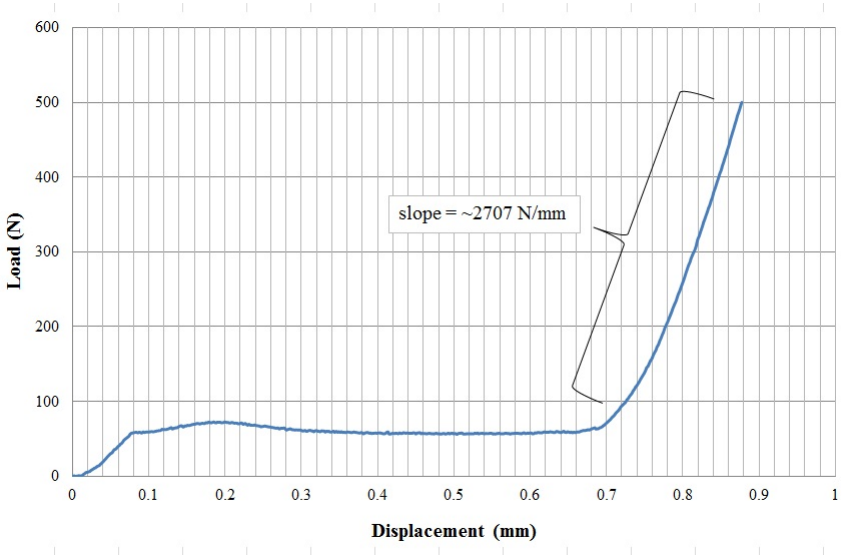


Figure 4.6: Load versus displacement curve for new casters

The general caster assembly consists of a cylindrical rod that can be slid into the vertical posts of the rack, the rod is then fastened with a bolt. The rod has a threaded end that a aluminum top plate is attached to. The aluminum top plate provides the top support for the isolators. The lower portion of the assembly consists of the caster and an aluminum plate that allows for the bottom support of isolators. The general assembly is shown in Figure 4.7

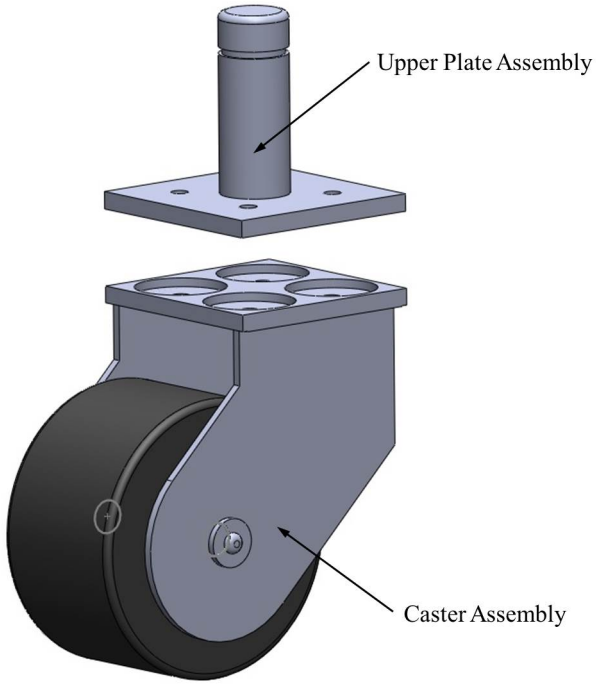


Figure 4.7: General isolation system assembly

The general assembly was chosen because of the ease it allows in interchanging isolators and the minimal maintenance required in the future, as compared to having ground pads or an active system. Having an isolator in the between the ground vibrations and the rack is easier to model because the assumed simple model of Equation 4.2 is directly represented. The general assembly allows for easy replacement of the isolator device should one be required.

#### 4.3.2.1 Metal Springs

Metal springs are comprised of thin coiled steel which can be manufactured in a wide range of diameters and lengths. The spring stiffness is dependent on the material of which it is comprised, the number of coil per measure of length, the diameter of the coil, and the diameter of the metal wire. The stiffness can be calculated using Equation 4.4 [33].

$$k = \frac{Gd^4}{8D^3 n_a} \tag{4.4}$$

In Equation 4.4 above, $G$ is the shear modulus of the metal, $d$ is the wire diameter, $D$ is the nominal coil diameter, and $n_a$ is the number of active coils. Metal springs have numerous positive aspects: they can isolate against large static deflections, exhibit nearly zero creep, have linear load versus displacement behavior, are insensitive to high and low temperatures, and their dynamic and static loading characteristics do not differ to any large extent [33]. However, metal springs do have any appreciable damping characteristics, which is a substantial shortcoming [33, 28, 30]. Systems isolated solely with metal springs are at risk of vibrations of structurally damaging amplitudes. If the resonance occurs in a system with very low damping, the amplitudes of the vibrations will reach much higher values than systems with high damping. In relation to animal racks, the excessive amplitudes may, depending on the circumstances, create for excessive physical discomfort for the animals located on the racks.

The lack of damping characteristics exhibited by metal coil springs and possible instability in lateral loading were reason enough to eliminate them from initial consideration as an isolation method for the mouse rack. Methods involving coil springs will be further considered if other methods are deemed inadequate. It is possible to combine the coil spring with a damping element or obtain a coil spring made out of a shape alloy which contains enhanced damping properties. However, it is more logical to pursue a system, especially because cost is of concern, that will contain the required stiffness characteristics and inherent damping capabilities.

#### 4.3.2.2 Helical Wire/Cable

Helical wire, also referred to as cable, isolators are comprised of metal wire wound in a helical pattern between two plates. The loops create for the stiffness characteristics of the isolator in compression and shear. Helical cable isolators are used in high intensity vibration applications with harsh environmental conditions and high/low temperatures [33, 28]. Figure 4.8 displays a helical wire isolator.

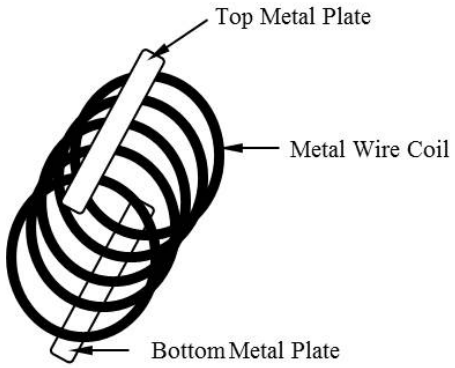


Figure 4.8: Helical wire isolator

The isolators exhibit non-linear softening behavior in compression though have nearly linear behavior in roll and shear [28]. Helical wire isolators have damping characteristics that are based on the internal friction that occurs between the strands in the wire coils. The damping within the isolators can be characterized to be of the Coulomb type [33]. Depending on the material of the cable, helical wire isolators can have a high resistance to corrosive environments and allow for large load ratings. The negative aspects of these isolators include their non-linear behavior and lack of versatility of isolator properties. The non-linearity of the isolators exist due to changes which occur as the strands of wire are compressed together at increasing loads; therefore, the isolator behavior is more difficult to model as compared to metal springs. Helical isolators are not available in as many configurations, load ratings, and stiffnesses as are their elastomeric counterparts. Though helical isolators could serve as a viable options for isolating the rack, they seem to not be the most versatile choice, which is critical when considering market availability of products and high sensitivity, laboratory applications. The pneumatic and elastomeric isolator were therefore considered to be better options in regards to this study.

#### 4.3.2.3 Pneumatic Isolators

Pneumatic isolators usually feature a metal foundation and an elastomeric body/air chamber. The body can be made of materials such as natural or neoprene rubber. The isolators contain a valve which provides an inlet for the elastomeric inflation chamber.

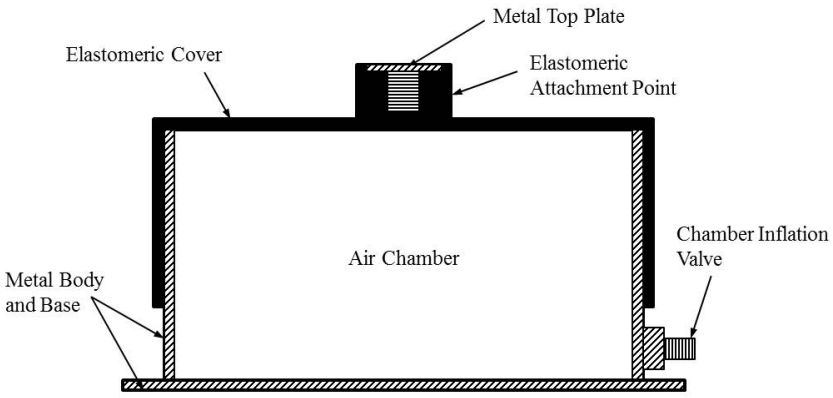


Figure 4.9: Pneumatic elastomeric isolator

Some pneumatic isolators contain a metal body with a rubber top cover which provides for the elastic expansion capabilities. Figure 4.9 displays a cross section of a sample pneumatic isolator.

Pneumatic isolators are well suited for low natural frequencies and are used in applications ranging from vehicle suspension systems, stationary machinery, and precision equipment [33, 28]. The pneumatic isolators provide a minimal level of damping and have an adjustable stiffness, which depends on the loading and internal pressure [33]. Pneumatic isolators have non-linear load versus displacement behavior starting with an initially steep slope which levels off to a nearly zero slope plateau and then becomes steep once more after a certain load. The relative stiffness behavior can be represented by Equation 4.5 [28].

$$k = pmg\frac{A}{V_o} \tag{4.5}$$

In Equation 4.5 above, $p$ is the specific heat ratio for air, $m$ is the mass of the system, $g$ is acceleration due to gravity, $A$ is the load supporting area of the air spring, $V_o$ is the air volume within the air chamber. However, the stiffness of the pneumatic isolator is not well represented by Equation 4.5 because of the highly variant behavior properties of the spring. Instead, to properly characterize the spring, it is best to develop a design chart by experimentally finding the load versus displacement curves of the pneumatic isolator at different pressures. The pneumatic isolator seemed like a highly viable option for the

task at hand, especially since pneumatic isolators are used in mitigating vibrations of highly sensitive equipment in science facilities. There are, however, several questions that arose in regards to utilizing a pneumatic isolator for mouse rack applications.

Two major factors were under question in relation to the pneumatic isolator: the range of adjustability and the vertical/horizontal stability. The range of stiffness adjustability in a pneumatic spring is difficult to quantify analytically due to the nonlinear behavior of the spring and also its dependence on internal pressure and applied load. However, the range of adjustability is important in order to determine the amount the stiffness can be varied with a certain device, prior to having to change the entire system altogether. The lateral and horizontal stability is critical in regards to the rack applications because the rack will not be stationary at all times and the isolation device may experience shear loads in addition to compressive forces. Limited information exists on all major manufacturer's websites and specification sheets. The maximum pressure and load are specified, as are product dimensions and materials used; however, some critical values are not given: the thickness of the elastomeric material or the metal wall, the maximum sustainable load in bending, load versus displacement curves, and damping characteristics. In order to properly design an isolation system with pneumatic isolators, an isolator had to be purchased and tested.

Characterization of a pnuematic isolator had to be done experimentally in order to obtain the necessary information for the system design. Cost constraints limited the selection of a pneumatic isolator as did the notion of having a high quality product. Numerous manufactures/distributors were contacted until the best possible pneumatic isolator was found for the cost restriction that was enforced. The isolator was purchased from McMaster-Carr, a distributor with a reputation for high quality products. The given isolator specifications are listed in Table 4.3 [20].

Table 4.3: Pneumatic isolator specifications

| **Parameter** | **Value** |
|---|---|
| Thread | M10 |
| Maximum Static Capacity per Mount | 448 N |
| Maximum Deflection | 12.7 mm |
| Maximum pressure | 414 kPa |
| Durometer | 65A |
| Overall Height | 63.5 mm |
| Outside Diameter | 73.4 mm |
| Square Base Size | 76.2 mm |
| Overall Height | 63.5 mm |
| Temperature Range | $-29°$ to $82°$ C |
| Elastomeric Material | Black Rubber |
| Body/Base Material | Aluminum |

Figure 4.10 is from McMaster-Carr and is a display of the pneumatic isolator. The isolator is similar in construction to the sample schematic shown in Figure 4.9.

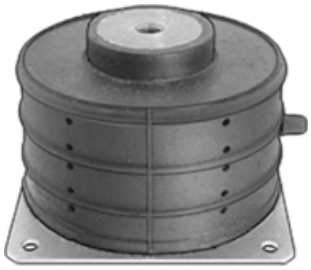

Figure 4.10: Pneumatic elastomeric isolator. Courtesy of McMaster-Carr.

Instead of using Equation 4.5, the stiffness of the pneumatic isolator was found experimentally by creating load versus displacement curves for the pneumatic isolator at different pressures. The load versus displacement curves were generated with the use of the Instron mechanical testing system. Figure 4.11 is a plot of the resulting load versus

displacement curves.

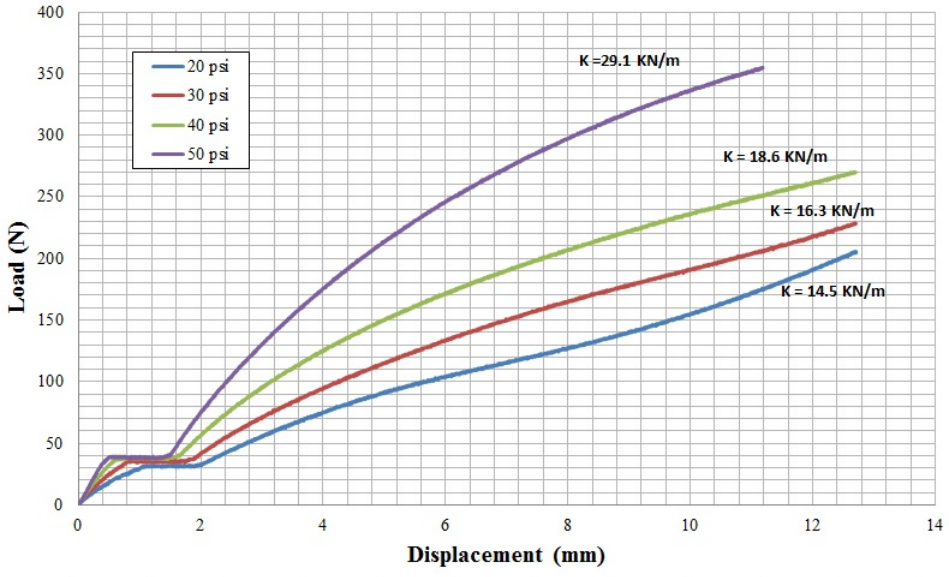


Figure 4.11: Pneumatic elastomeric isolator load versus displacement plot

In Figure 4.11, the portions of the curves after approximately 2 mm are assumed to be linear and stiffness values are developed for each curve based on this assumption. The increasing slope portion tends to happen after about 50 N, the self-weight of the rack will load each isolator more than 50 N; therefore, the values of the sloped portion after the plateau were used to determine stiffness values for the isolator. The stiffness values could then be used with Equation 4.2 in order to determine if the transmissibility of the system will meet or be below the desired transmissibility goal of 0.66. All of the stiffness values were used to calculate the respective transmissibility at the medium load value. The transmissibility values are calculated using Equation 4.2 and the equivalent stiffness value of the casters. The results are given in Table 4.4. The stiffness in Table 4.4 is based on the stiffnesses determine from Figure 4.11 multiplied by four in order to account for an isolator on each caster.

Table 4.4: Stiffness and transmissibility characteristics of pnuematic isolator

| **Stiffness (KN/m)** | **Transmissibility** |
|---|---|
| 14.5 | 0.05 |
| 16.3 | 0.06 |
| 18.6 | 0.07 |
| 29.1 | 0.11 |

All of the stiffnesses in Table 4.4, when paired with the medium rack loading, yield a transmissibility below the required value. The stiffness values in Table 4.4 are multiplied by four prior to using the transmissibility equation, in order to account for the four casters. However, this is only one of the isolator selection criteria. The range of transmissibility values is not very high, meaning that though the pressure within the isolator can increase from 20 to 50 psi, the return in added stiffness does not greatly affect the overall system response. Conclusion: the pneumatic caster has a fairly low adjustability. Next, estimates of natural frequencies were calculated using each of the stiffness values in order to determine if they correlate with the forcing frequencies. If the estimated natural frequencies are the same as the ground forcing frequencies, the system may have problems with resonance. Table 4.5 displays the natural frequencies of the system.

Table 4.5: Natural frequencies of pneumatic isolator system

| **Stiffness (KN/m)** | **Natural Frequency (rad/s)** | **Natural Frequency (Hz)** |
|---|---|---|
| 14.5 | 25.0 | 3.98 |
| 16.3 | 26.5 | 4.22 |
| 18.6 | 28.3 | 4.51 |
| 29.1 | 35.4 | 5.64 |

The stiffness values in Table 4.5 are multiplied by four prior to using the natural frequency equation, in order to account for the four casters. The natural frequencies

seem high enough as to not cause resonance issues with the very low portion of the ground vibrations (6.28 to 12.56 rad/s). The largest possible stiffness value is going to be used in the design to limit effects due to resonance. Once a stiffness value was selected, the vertical and horizontal stability of the isolator was tested by securing the pneumatic isolators to the general assembly casters and fastening the caster assembly on an empty rack. The vertical load capacity of the isolators is well within the load produced by the self-weight of the rack; however, the casters are offset from the center of the rack rods, which creates for a moment at the top of the caster assmebly. A diagram of the caster and the moment is shown below in Figure 4.12.

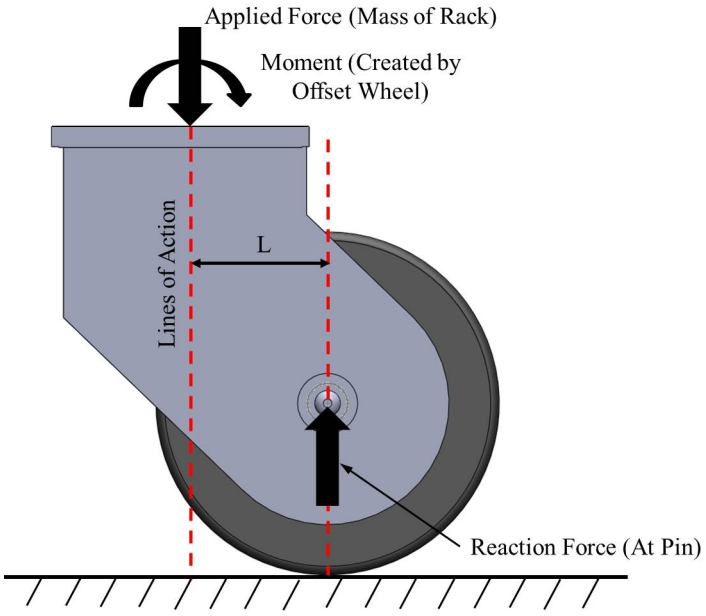


Figure 4.12: Moment being generated due to rack loading

The moment that is created about the top of the caster assembly creates for a minimal bending resistance that needs to be met by the isolator. The design of the isolator makes it extremely susceptible to bending deflections because, as the air chamber become pressurized, the elastomeric attachment portion of the isolator is pushed upward and all of the bending is resisted only by a small portion of air and rubber. This was unknown and incalculable prior to purchase of the isolator. The physical test of fastening the

retro-fitted caster assembly onto the rack resulted in near-catastrophic failure of the isolators. The isolators immediately bent laterally due to the load of the rack and had little stability. This test proved that the pneumatic isolators, with the current design, are not suitable as vibration mitigation method for the rack. Aside from the lateral instability, other inconveniences were found to exist with pneumatic isolators.

The pnuematic caster assembly has other potential issues in addition to poor resistance to shear forces, the main two being: temperature dependent expansion and natural system frequencies which are low and may cause resonant behavior to occur. The pressure dependence on temperature is critical, especially because the racks will be going through a hot wash, which will cause the air in the pneumatic isolators to expand. If the pressure is too great within the isolator, it may burst and lose its effectiveness as a mitigation device. The pneumatic isolator greatly lowers the natural frequency of the system due to the low stiffness values it allows for; however, a low natural frequency may create for resonance within the system should the stiffness of the casters drop. A drop in air pressure will result in a drop in stiffness; hence, the isolators will have to be constantly checked to see if they maintain adequate pressure. The pnuematic isolator was not effective as a mitigation device and the last mitigation device type was considered - elastomers.

#### 4.3.2.4 Elastomers

Elastomers were the last mitigation device type considered and are one of the most simple to implement and maintain. Elastomers come in many configurations and have a wide range of material properties. Most elastomeric materials exhibit non-linear material behavior. The stiffness of the elastomers may change depending on the loading frequency and if the load versus displacement curve is linear only under a small portion of the loading. Elastomers have energy dissipative capabilities and convert mechanical energy into heat energy through internal friction between planes within the material [30]. The load versus displacement response of a elastomeric material can represented by Figure 4.13.

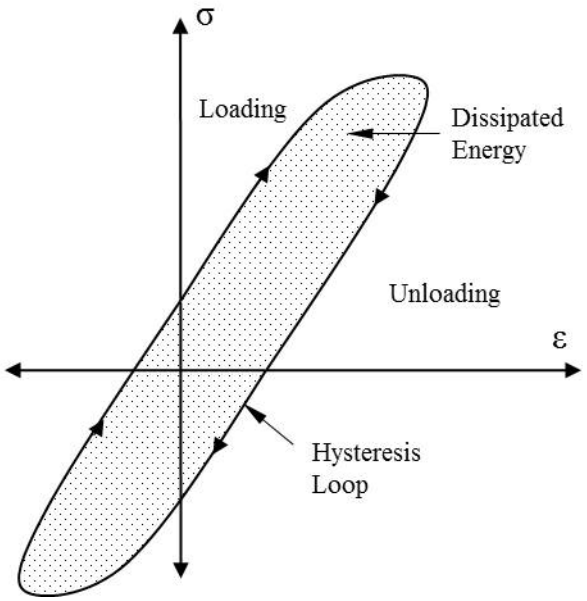


Figure 4.13: Example load versus displacement plot of a typical elastomeric material, hysteresis is noted. As adapted from [30]

In Figure 4.13, the loading path of the material differs from the unloading path. The area in between the loading and unloading portion of the curve is the strain energy that is lost in the process, the energy that is dissipated as heat. The behavior exhibited in Figure **??** is referred to as hysteresis and is a representation of the damping capabilities of the material. Elastomeric materials can have a relatively high damping which aids in limiting peak vibrations during resonance. Elastomers may be formulated to have a relatively large tolerance for high temperatures and chemical attack. The versatility of elastomers makes them great candidates for vibration isolation.

There is a myriad of data available from manufactures for elastomeric mounts and pads, possibly because of their wide use and easy load versus displacement characterization in quasi-static loading situations. Elastomeric ground pads were considered as a mitigation device because of their ease of use and the lack of manufacturing that is necessary to make them adaptable to the caster system. However, pads will quickly become dirty and will require thorough cleaning in order to make them suitable for the clean laboratory setting. The extra work of moving the rack and cleaning the pads

is inconvenient. The pads also do not have a defined load versus displacement curve because pressure on the pads depends on the area that is compressed by the casters, which will change with the amount of loading on the rack. Elastomeric mounts, though, have a defined load versus displacement because of their predetermined, fixed shape and also will require no extra cleaning. Elastomeric mounts were found which fit well with the general caster assembly and which have the necessary stiffness characteristics. The elastomeric mount designation is V10Z 2M310AM08 and was purchased from the company: Advanced Antivibration Components [1]. A diagram with isolator dimensions is displayed in Figure 4.14 [1]. The stiffness characteristics of several types of single elastomeric mounts are shown in Figure 4.15. The load versus displacement curve of the isolator selected for this study is curve **A**.

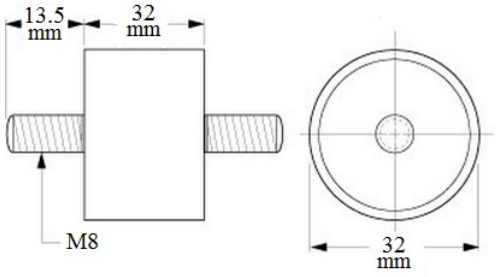


Figure 4.14: Selected elastomeric isolator. Courtesy of Advanced Antivibration Components.

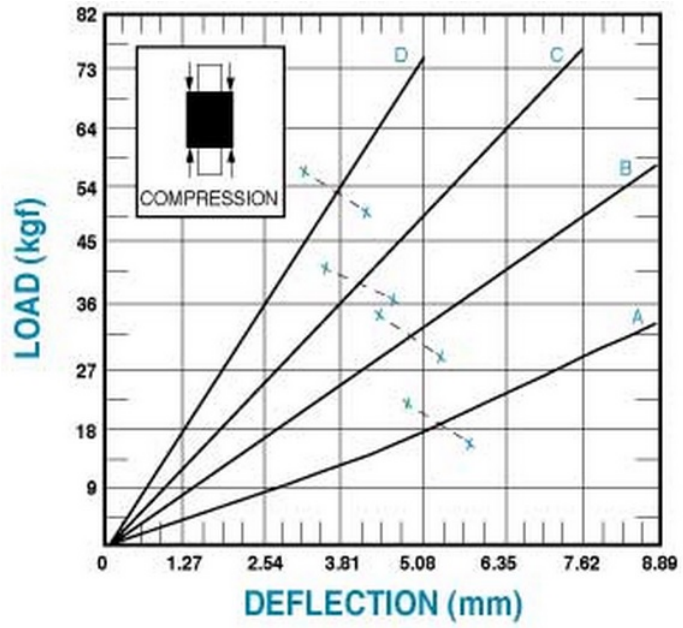


Figure 4.15: Load versus displacement curves for elastomeric mounts. Courtesy of Advanced Antivibration Components.

A combination of four Type A elastomeric mounts was chosen for a single caster assembly. The combined stiffness of four of the Type A mounts equals approximately 135 KN/m. The calculated transmissibility ranges from 0.51 to 0.84 for the high and medium load, respectively. The transmissibility values exceed the goal of 0.66 when the rack is highly loaded but do not quite meet it when the rack is at a medium load; however, approximately 12 kg of mass can be added to the medium loaded rack to reach the benchmark. In regards to structural stability, the system also meets all of the necessary requirements. The three combined mounts can sustain a maximum static compressive load of 74.4 kg ( 730 N) and a shear load of 38 kg ( 373 N) [1]. The maximum vertical load that the rack will experience per caster is 307 N. In order to access the load carrying capabilities of the isolators, the offset of the caster needed to be taken into account. The calculations that were conducted were based on the diagram in Figure 4.12 and the maximum moment and vertical force that the mounts will experience from a highly loaded rack was determined. The free body diagram in Figure 4.16 was used to represent the forces on the caster and ultimately the force that the isolators

would need to resist in bending.

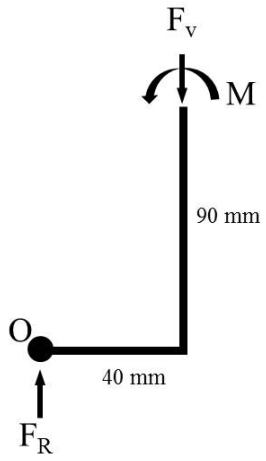


Figure 4.16: Free body diagram of a single caster

In Figure 4.16, moments were summed about point $O$ in order to find moment $M$. The calculations result in $M$ being 12.3 N-m, which was then used in a beam bending calculation in order to determine the maximum load carrying capabilities of the system. The structural calculations are shown in *Appendix B*. The requirements for stability and stiffness are satisfied based on the calculations. The elastomeric mounts are made of natural rubber which has a temperature range of -51 to 104 degrees Celsius [10], this satisfies the temperature criteria. The natural frequency of the system varies between 11.4 and 12.2 Hz for the high and medium load, respectively. The natural frequencies values do not coincide with any major forcing frequencies and thus should not create for major resonance problems in the system. The only criteria that the elastomeric mounts do no satisfy is that of adjustability; however, mass can be added to the rack in order to change the characteristics of the system or a new set of mounts can be selected to fill any new isolation requirements. All calculations were done in Matlab using the script in Appendix A and B. Exchanging the mounts with another set will not be difficult so long as the threads on the new mounts are the same as the previous mounts. The final elastomeric mount assembly is shown in Figure 4.17

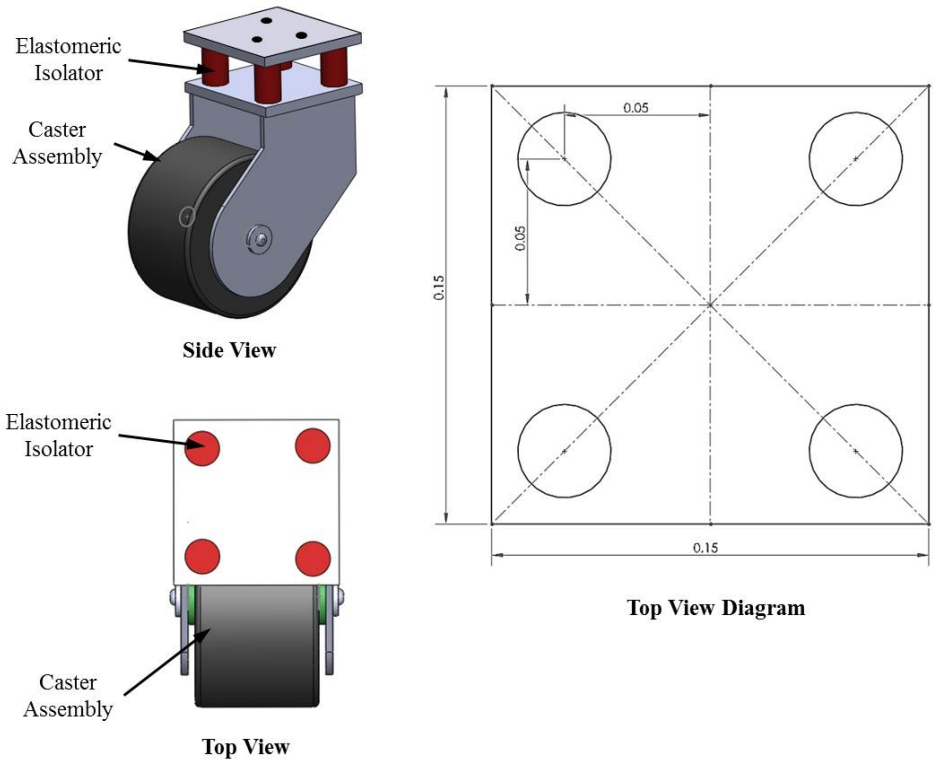


Figure 4.17: Final elastomeric isolator assembly

It is important to note that the assembly in Figure 4.17 does not have a rod attachment like that of the pneumatic spring system. The caster system in Figure 4.17 will be attached on the underside of the cart as opposed to at the rods in order to provide for a more compact system. If the caster assemblies were to be fastened to the rods, the assemblies would protrude from the frame of the rack and could catch on doorways or on other racks in the room when the retrofitted rack is moved.

## 4.4 Future Work and Suggestions

The elastomeric isolator design will need to be physically fabricated and tested on the rack. The test can be conducted by simply measuring the vibrations on the new, retrofitted system and determining if adequate isolation occurs when the train passes the LARC. Using video footage, if the train is observed to pass the facility, and no vibrations are measured which extend beyond the ambient level of vibrations, then the system can be deemed a success. If the system does not perform as designed, an assessment will have to be conducted of the fabricated components, the governing design equations, and the assumptions that were made. Future work can be conducted by undergraduate or graduate students to develop a more optimized vibration isolation system.

This study has lead to several conclusions, among them being that designing vibration isolation systems is not a trivial task. Many assumptions have to be made and it is difficult to characterize any system with complete accuracy. Many times, interactions will occur between multiple vibration sources or a vibration source will promote amplification of vibration in a broad frequency range. The latter behavior was observed in this study: with the passing of the train, a set of vibrations within a range of frequencies became present. Having a wide set of frequencies present creates for difficulty in determining which vibration frequencies are most dominate and which should be used in the isolation design. Furthermore, if a design is selected to encompass a set frequency range, the impacts to the system need to be assessed if vibrations occur beyond the scope of the design. The surrounding environment may also change and, even if there was an ideal isolation solution found, it may no longer suffice. Therefore, great care has to be taken in assessing the vibrations impacting a system and multiple iterations need not be viewed as failures, but instead as design optimization. Creating a vibration isolation system which function well in between a caster and a mass further complicates the situation. Bending load requirements become critical in moving systems because they are not solely being loaded in a vertical manner. In order to conduct a proper system assessment and future system optimization, good quality equipment is required as is a proper facility.

For future studies it will be ideal to have multiple high sensitivity, three-axis accelerometers. The accelerometer used in this study may have created for too much noise due to its sensitivity level, higher sensitivity accelerometers will allow for more accurate vibration characterization. Obtaining a professional, high-quality electromagnetic

shaker will also be of great benefit. The professional electromagnetic shaker will provide for more power in exciting the system than was available with the subwoofer assembly created for this study. Ideally, a platform could be built which would support the rack and have the electromagnetic shaker present underneath. In this way, the entire system could be exposed to any desired set of vibrations and the train vibrations would be simulated in a controlled setting. Aside from equipment, a proper facility is needed in which very limited vibrations occur. If a facility is prone to a wide variety of vibrations, they may interfere when system assessments are made and add complexity to determining which vibrations are from the source in question.

# Chapter 5: Conclusion

## 5.1 Summary of Work

Poor reproductive success among mice means that investigators must use more animals, at greater expense, to complete their research studies. Experimental outcomes can be skewed due to increased, vibration induced stress in the mice [2, 9, 18, 26]. The preliminary data gathered at OSU reveals that vibrations can be a deleterious factor in respect to the reproductive success of mice on flat racks. Some of the largest vibrations encountered in room 103 in the LARC have been identified to originate from the passing of a train.

In order to quantitatively categorize the effect of train vibrations on mice, stress levels were measured by conducting FCM analyses using vibrated groups of male and female mice. The vibration was induced through a custom-built electromagnetic shaker device which mimicked the vibrations produced by trains passing near the LARC. Measuring the stress levels in several groups of male and female mice offered insight into the effect of the vibrations and serves as a baseline upon which to conduct future studies. It was established that vibrations from the passing trains create fluctuations in the corticosterone levels of mice. Fluctuations in stress levels may be extremely disruptive in studies where stress may negatively influence research outcomes. Elevated corticosterone levels can induce a variety of ill effects in rodents, including a lower reproductive success rate [2, 35, 36, 39, 40]. Research should be extended to quantify the range of vibrations experienced at different locations within the same building and to buildings constructed to varying standards. The more knowledge that is gathered about the types of vibrations that exist in animal facilities, the easier it will be to mitigate the impacts caused by the vibrations.

## 5.2 Impact of Study

The importance of this study lies in that it raises awareness in regards to an issue that is present in nearly every animal laboratory in the United States, yet is completely neglected. The study verifies the hypothesis that environmental vibrations may cause distress within animals as noted by fluctuations in FCM levels. Furthermore, the latter part of the study explores options for mitigating high amplitude vibrations from a specific environmental source. This thesis has been written with the laboratory animal researcher in mind - care has been taken to explain all mechanical engineering concepts plainly and in a manner which anyone with a scientific background can understand. The methods and conclusions stated herein can serve as a starting point for a more intensive investigation into any of the aspects of this study, whether they be a comprehensive study of stress levels within mice when exposed to various environmental vibrations or a revolutionary vibration mitigation device specifically designed for laboratory rack applications.

## 5.3 Final Remarks

In summary, it can be concluded that the issue of environmental vibrations is one of considerable complexity. It is difficult to quantify the exact impact that vibrations have on the biological workings of mice and the extent of the detriment they pose to laboratory studies involving animals. Vibrations are present in every facility, and much more so in facilities located near trains and possibly large highways, airports, subways, and construction zones. Thus, the measurement of vibration magnitudes and frequencies should be a paramount objective of any laboratory animal science facility. With more awareness drawn to environmental vibrations, more studies will be conducted to examine the impacts vibrations have on laboratory research and the physiology of the animals that experience them.

# Bibliography

[1] Cylindrical mounts, May 2014.

[2] M. Arizumi and A. Okada. Effect of whole-body vibration on the rat brain content of serotonin and plasma corticosterone. *European Journal of Applied Physiology and Occupational Physiology*, 52:15–19, 1983.

[3] A. L. Baldwin. Effects of noise on rodent physiology. *International Journal of Comparative Psychology*, 20:134–144, 2007.

[4] H.T. Banks and G.A. Pinter. Damping: Hysteretic damping and models. In D. Ewins and S.S. Rao, editors, *Encyclopedia of Vibration*.

[5] A. Barber. *Handbook of Noise and Vibration Control*. Elsevier Advanced Technology, 1992.

[6] I. Bernatova, M. P. Key, J. B. Lucot, and M. Morris. Circadian differences in stress-induced pressor reactivity in mice. *Hypertension*, 40:768–773, 2002.

[7] M. M. Constantine, F. Ferrari, G. Chiossi, E. Tamayo, G. D. Hankins, G. R. Saade, and M. Longo. Effect of intrauterine fetal programming on response to postnatal shaker stress in endothelial nitric oxide knockout mouse model. *American Journal of Obstetrics and Gynecology*, 201:301–316, 2009.

[8] National Research Council. *Guide for the Care and Use of Laboratory Animals*. The National Academies Press, Washington, D.C., 2011.

[9] F. S. Dhabhar, A. N. Saul, T. H. Holmes, C. Daugherty, E. Neri, J. M. Tillie, D. Kusewitt, and T. M. Oberyszyn. High-anxious individuals show increased chronic stress burden, decreased protective immunity, and increased cancer progression in a mouse model of squamous cell carcinoma. *PLoS One*, 7:1–14, 2012.

[10] Properties of rubber compounds, May 2014.

[11] Upseis an educational site for budding seismologists, 2013.

[12] H. Hashiguchi, S. H. Ye, M. Morris, and N. Alexander. Single and repeated environmental stress: effect on plasma oxytocin, corticonsterone, catecholamines, and behavior. *Physiology and Behavior*, 61:731–736, 1997.

[13] H. E. Heffner and R. S. Heffner. Hearing ranges of laboratory animals. *Journal of American Association for Laboratory Animal Science*, 46(1):20–22, 2007.

[14] L. F. Hughes. The fundamentals of sound and its measurement. *Journal of the American Association for Laboratory Animal Science*, 46:14–19, 2007.

[15] Daniel J Inman. *Engineering vibration*. Prentice Hall, 3 edition, 2007.

[16] K. Jensen, N. E. Hahn, R. Palme, K. Saxton, and D. D. Francis. Vacuum-cleaner noise and acute stress responses in female c57bl/6 mice (mus musculus). *Journal of the American Association for Laboratory Animal Science*, 49:300–306, 2010.

[17] E. W. Kamen. *Fundamentals of Signals and Systems Using the Web and MATLAB*. Prentice Hall, 2006.

[18] W. Lane-Petter. Cannibalism in rats and mice. *Proceedings of the Royal Society of Medicine*, 61:1295–1296, 1968.

[19] N. Lipman, J. Fox, S. Barthold, M. Davisson, C. Newcomer, F. Quimby, and A. Smith. *The Mouse in Biomedical Research: Normative Biology, Husbandry, and Models*. Academic Press, San Diego, 2007.

[20] Inflatable high-deflection vibration-damping mounts, May 2014.

[21] M. A. Montenegro, H. Palomino, and H. M. Palomino. The influence of earthquake-induced stress on human facial clefting and its simulation in mice. *Archives of Oral Biology*, 40:33–37, 1995.

[22] D.C. Montgomery. *Design and Analysis of Experiments*. Wiley, 2012.

[23] T. Nakata, W. Bernard, E. Kogosov, and N. Alexander. Cardiovascular change and hypothalamic norepinerphine release in response to environmental stress. *The American Journal of Physiology - Regulatory, Integrative and Comparative Physiology*, 264:R784–R789, 1993.

[24] Interactive sound ruler, July 2013.

[25] Labview measurements manual, 2003.

[26] J. N. Norton, W. L. Kinard, and R. P. Reynolds. Comparative vibration levels perceived among species in a laboratory animal facility. *Journal of the American Association for Laboratory Animal Science*, 50:653–659, 2011.

[27] A. T. Peplow, C. J. Jones, and M. Petyt. Surface vibration propagation over a layered elastic half-space with an inclusion. *Applied Acoustics*, 56:283–296, 1999.

[28] A.G. Piersol and T.L. Paez. *Harris' Shock and Vibration Handbook*. McGraw-Hill, New York, 6 edition, 2010.

[29] K. D. Randall. *Physics for Scientists and Engineers: A Strategic Approach with Modern Physics and MasteringPhysics*. Addison-Wesley, 2007.

[30] Singiresu S Rao. *Mechanical vibrations*. Addison-Wesley Publishing, 3 edition, 1995.

[31] S. Rasmussen, G. Glickman, R. Norinsky, F. W. Quimby, and R. J. Tolwani. Construction noise decreases reproductive efficiency in mice. *Journal of the American Association for Laboratory Animal Science*, 48:363–370, 2009.

[32] R. P. Reynolds, W. L. Kinard, J. J. Degraff, N. Leverage, and J. N. Norton. Noise in a laboratory animal facility from the human and mouse perspectives. *Journal of an American Association for Laboratory Animal Facility*, 49(5):592–597, 2010.

[33] E.I. Rivin. *Passive Vibration Isolation*. ASME Press, New York, 2003.

[34] C. T. Rubin, E. Capilla, Y. K. Luu, B. Busa, H. Crawford, D. J. Nolan, V. Mittal, C. J. Rosen, J. E. Pessin, and S. Judex. Adipogensis is inhibited by brief, daily exposure to high-frequency, extremely low-magnitude mechanical signals. *Proceedings of the National Academy of Sciences*, 104:17879–17884, 2007.

[35] A. M. Sackler and A. S. Weltman. Effects of vibration on the endocrine system of male and female rats. *Aerospace Medicine*, 37:158–166, 1983.

[36] M. A. Toraason, D. W. Badger, and G. L. Wright. Gastrointestinal response in rats to vibration and restraint. *Environmental Research*, 23:341–347, 1980.

[37] C. Toumaa, R. Palme, and N. Sachsera. Analyzing corticosterone metabolites in fecal samples of mice: a noninvasive technique to monitor stress hormones. *Hormones and Behavior*, 45:10–22, 2004.

[38] D. J. Wald, V. Quitoriano, T. H. Heaton, and H. Kanamori. Relationship between peak ground acceleration, peak ground velocity, and modified mercalli intensity in california. *Earthquake Spectra*, 15:557–564, 1992.

[39] L. Xie, J. M. Jacobson, E. S. Choi, B. Busa, L. R. Donahue, L. M. Miler, C. T. Rubin, and S. Judex. Low-level mechanical vibrations can influence bone resorption in the growing skeletion. *Bone*, 39:1059–1066, 2006.

[40] L. Xie, C. Rubin, and S. Judex. Enhancement of the adolescent murine musculoskeletal system using low-level mechanical vibrations. *Journal of Applied Physiology*, 104:1056–1062, 2008.

# APPENDICES

# Appendix A: Matlab Code

```
Clc
clear all
close all

k_o = 938000*4; % stiffness value for four original casters (KN/m)
m1 = 92.7; % kg
m2 = 125; % kg
w = 18*3.14*2; % ground vibration frequency (rad/s)
w_r = 14*3.14*2; % rack vibration frequency (rad/s)
a_r = .015*9.81; % rack acceleration (m/s^2)
a_g = .01*9.81; % ground acceleration (m/s^2)
T = 1.0;
k2_o = 938000*4; % stiffness value for four original casters (KN/m)
T2 = 1.0;
A_a = 0.004*9.81; % ambient reponse vibration maximum (m/s^2)

% Tranmissibility value calculated for the original system using different
% loads

T_m = abs(k_o/(k_o-m1*w^2)) % medium load
T_h = abs(k2_o/(k2_o-m2*w^2)) % high load
r1 = (w/sqrt(k_o/m1));
r2 = (w/sqrt(k2_o/m2)) ;

% Determining necesary tranmissibility values

A_r = (a_r/(w_r)^2)*1000 % maximum response displacements (mm)
A_g = (a_g/(w)^2)*1000 % maximum ground displacements (mm)
E_T = A_r/A_g % experimental transmissibility

% Calculation of ambient vibration displacement

A_a = (A_a/(w_r)^2)*1000 % maximum ambient response displacements (mm)
T_req = A_a/A_g % desired train transmissibility

% Iteration for determining the necessary system stiffness values for a
% transmissibility of .4

k = 900000 % starting stiffness value

while T >T_req
    T = abs(k/(k-m1*w^2));
    k = k - 1000;
end

k

k2 = 900000 % starting stiffness value

while T2 >T_req
    T2 = abs(k2/(k2-m2*w^2));
    k2 = k2 - 1000;
end

k2

% Transmissibility plots ////////////////////////////////////////////
```

```
% Transmissibility for medium load

k_c = [500000000:-1000:0]; % changing stiffness values
w_nm = sqrt(k_c./m1);  % changing natural frequency with medium load
r_m = w./w_nm ;
T_m2 = abs(k_c./(k_c-m1*w^2));

% Transmissibility for high load

k_c = [500000000:-1000:0]; % changing stiffness values
w_nm2 = sqrt(k_c./m2);  % changing natural frequency with medium load
r_h = w./w_nm2 ;
T_h2 = abs(k_c./(k_c-m2*w^2));

% Transmissibility Plot

set(0,'DefaultAxesFontName', 'Times New Roman')

plot(r_m,T_m2,'-k')
hold on
% plot(r_h,T_h2,'--k') % curve will be same as curve for m1
plot(r1,T_m,'or')
plot(r2,T_h,'ob')
grid on
legend('Medium and High Load Curve', 'System Transmissibility Medium Load',
'System Transmissibility High Load')
% hold on
% plot(r,1,'-k')

axis([0 4 0 6])

xlabel('Frequency Ratio r = \omega/\omega_n')
ylabel('Displacement Transmissibility T = |X/Y|')

%////////////////////////////////////////////

% Percent difference between analytical and experimental value

av = [E_T, T_m]
Percent_Diff = abs((E_T-T_m)/mean(av))*100

% Natural frequency determination of original system and system w/ pneumatic
isolators

wn_o_m = sqrt(k_o/m1); % natural angular frequency w/ medium mass on original
system
wn_o_h = sqrt(k_o/m2); % natural angular frequency w/ high mass on original
system
wn_n_m = sqrt(k/m1); % natural angular frequency w/ medium mass
wn_n_h = sqrt(k/m2); % natural angular frequency w/ high mass

fn_o_m = wn_o_m/(3.14*2) % natural frequency w/ medium mass on original
system
fn_o_h = wn_o_h/(3.14*2) % natural  frequency w/ high mass on original system
fn_n_m = wn_n_m/(3.14*2) % natural  frequency w/ medium mass
fn_n_h = wn_n_h/(3.14*2) % natural  frequency w/ high mass
```

```
% Tranmissibility determination of elastomeric isolator

K_c = 135 * 1000; % stiffness per caster (KN/m)
K_c_t = K_c * 4 ;% total stiffness of system (KN/m)
T_el_m = abs(k_c_t/(k_c_t-m1*w^2)) % medium load
T_el_h = abs(k_c_t/(k_c_t-m2*w^2)) % high load

% Natural frequency determination of elastomeric isolator

wn_el_m = sqrt((K_c*4)/m1); % natural angular frequency w/ medium mass
wn_el_h = sqrt((K_c*4)/m2); % natural angular frequency w/ high mass
fn_el_m = wn_el_m/(3.14*2) % natural  frequency w/ medium mass
fn_el_h = wn_el_h/(3.14*2) % natural  frequency w/ high mass
```

# Appendix B: Structural Stability Calculation - Elastomeric Isolator

Area Moment of Interia of Circle : $I_y = \pi r^4 / 4$

Radius of Isolators: 0.016 meters

## Max Stress Calculation

| Objects | Ai | yi | yi*Ai | Ii | $di=yi-y_{bar}$ | di^2*A |
|---|---|---|---|---|---|---|
| 1 | 0.0008 | 0.05 | 0.00004 | 5.14458E-08 | 0.05 | 0.000002 |
| 2 | 0.0008 | 0.05 | 0.00004 | 5.14458E-08 | 0.05 | 0.000002 |
| 3 | 0.0008 | -0.05 | -0.00004 | 5.14458E-08 | -0.05 | 0.000002 |
| 4 | 0.0008 | -0.05 | -0.00004 | 5.14458E-08 | -0.05 | 0.000002 |
| **Sum** | 0.0032 | | 0 | 2.05783E-07 | | 0.000006 |

| | |
|---|---|
| $y_{bar}$ | 0 |
| I | 6.2E-06 |
| c | 0.066 |
| M (N*m) | 12.3 |
| $\sigma_{max}$ (kPa) | 131 |
| $P_{max}$ (N) | 1200 |
| $S_{max}$ (kPa) | 375 |
| $F_{max}$ (N) | 307 |
| $\sigma_{vertical\ max}$ (kPa) | 96 |
| $\sigma_{total}$ (kPa) | 227 |
| Safety Factor | 1.7 |

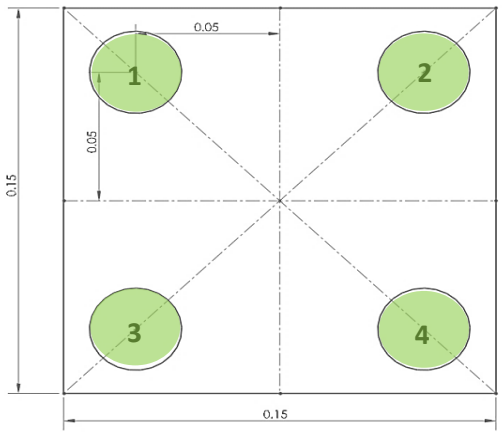


Figure 1. Highlighted green objects represent isolator areas

$y_{bar}$ - caculated centroid

I - total moment of interia

c - distance from centroid to point farthest away

M (N*m) - maximum calculated moment

$\sigma_{max}$ (kPa) - maximum calculated compressive stress

$P_{max}$ (N) - maximum load isolators can sustain

$S_{max}$ (kPa) - maximum stress isolators can sustain

$F_{max}$ (N) - Maximum vertical force applied to each caster

$\sigma_{vertical\ max}$ (kPa) - maximum vertical stress applied to each caster

$\sigma_{total}$ (kPa) - total stress resulting from generated moment and vertical force

Safety factor - the maximum stress the combined isolator system can sustain over the maximum stress that will applied to each caster

* It is important to note that the Pmax value used is that if the system encountered a dynamic event. The safe static load is ~730 N which will make the percent difference approximate .6. However, the system will rarely see a maximum vertical load of 307 N and thus the moment and the vertical force will almost always be lower than as presented here. The dynamic capabilities of the isolators will allow for a safety factor of ~1.7

## Buckling

| | |
|---|---|
| L (m) | 0.032 |
| r | 0.044 |
| L/r | 0.7 |

L - length of isolators

r - total moment of interia

c - distance from centroid to point farthest away

very small slenderness ratio; therefore, most likely no buckling will occur